PCCP

www.rsc.org/pccp

PERSPECTIVE

Molecular optoelectronics: the interaction of molecular conduction junctions with light

Michael Galperin[a] and Abraham Nitzan*[b]

The interaction of light with molecular conduction junctions is attracting growing interest as a challenging experimental and theoretical problem on one hand, and because of its potential application as a characterization and control tool on the other. It stands at the interface between two important fields, molecular electronics and molecular plasmonics and has attracted attention as a challenging scientific problem with potentially important technological consequences. Here we review the present state of the art of this field, focusing on several key phenomena and applications: using light as a switching device, using light to control junction transport in the adiabatic and non-adiabatic regimes, light generation in biased junctions and Raman scattering from such systems. This field has seen remarkable progress in the past decade, and the growing availability of scanning tip configurations that can combine optical and electrical probes suggests that further progress towards the goal of realizing molecular optoelectronics on the nanoscale is imminent.

1. Introduction

The interaction of molecular conduction junctions with light has long been perceived as an obviously needed development in this field, for several important reasons. First, *characterization* is a standing issue in the field, where much relies on properties

[a] *Department of Chemistry and Biochemistry, University of California at San Diego, La Jolla, CA 92093, USA. E-mail: migalperin@ucsd.edu*
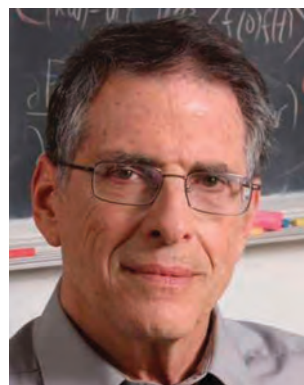[b] *School of Chemistry, Tel Aviv University, Tel Aviv, 69978, Israel*

of molecular species bridging between metal or semiconductor leads but little is known about the structure (or structures) involved in the conduction process to the extent that sometimes even the existence of a molecular bridge between the leads is uncertain. Inelastic electron tunneling spectroscopy, from which information about junction structures is obtained from their vibrational fingerprints, is arguably the most important characterization tool used today. Raman spectroscopy would provide equivalent information, with the added benefit of incoming and outgoing frequencies resolution. Other linear

Michael Galperin graduated with MSc in Theoretical Physics from Ural State University, Russia, in 1991. He earned a PhD in Chemical Physics in 2003 at Tel Aviv University under the supervision of Prof. Abraham Nitzan. After postdoctoral positions at Duke University in 2002–2003, Northwestern University in 2003–2007, and Los Alamos National Laboratory in 2007–2008, in 2008 he joined the faculty at University of California, San Diego

Michael Galperin

where he is currently an assistant professor of Chemistry and Biochemistry. He is interested in quantum transport, excitation, dissipation and relaxation processes in open non-equilibrium molecular systems.

Abraham Nitzan is a professor of Chemistry and the director of the Sackler Institute of Advanced Studies at Tel Aviv University. His research focuses on theoretical aspects of chemical dynamics, in particular the interaction of light with molecular systems and charge transfer processes in condensed phases and interfaces. Among his main recognitions are the Humboldt Award, the ICS Prize and the Israel Prize in Chemistry. He is a fellow of the American Physical

Abraham Nitzan

Society and of the American Association for the Advancement of Science, a Foreign Honorary member of the American Academy of Arts and Sciences and a member of the Israel Academy of Arts and Sciences. In 2010 he has received an honorary doctorate (Dr Honoris Causa) from the University of Konstanz.

and non-linear optical spectroscopies would in principle be similarly useful.

Second, light is potentially a control tool that can affect the junction conduction properties by inducing photophysical or photochemical processes that change the junction electronic structure and/or conformation. This can replace the more common practice of control by a gate potential, whose efficiency is much reduced in systems of nano-dimensions, while having the obvious advantages of speed and selectivity.

Third, typical junctions comprise dielectric structures (metal and/or semiconductor leads) whose dimensions are characteristic of systems that sustain localized surface plasmons – collective electronic oscillations that couple efficiently with the radiation field, and can give rise to strong focusing (implying strong intensity enhancement) and sub-wavelength resolution of electromagnetic effects. Indeed, the study of molecular junctions interacting with the radiation field lies at the juncture of two subjects that have attracted considerable attention and much experimental and theoretical effort in the past two decades: molecular electronics and molecular plasmonics.

From the theoretical perspective, understanding observations associated with the mutual interaction between molecular conduction junctions and the radiation field is a challenging endeavor. On one hand, the need to describe the optical response of a junction structure constitutes a complex problem in nano-plasmonics. On the other, the molecular response to the local radiation field, while seemingly a standard problem in linear or non-linear spectroscopy, now has the extra dimension stemming from the fact that the molecular system is open to electrons and, moreover, is in contact with electron reservoirs characterized by different electronic chemical potentials. The molecular subsystem is consequently in a non-equilibrium state that results from two different driving processes – an electron flux induced by an external potential bias and a photon flux associated with an incident radiation field. With a variation on the theme, one of these fluxes, rather than being externally induced, appears as a response to the other. Thus, we can encounter phenomena where light appears in response to electrical driving (bias potential) or, conversely, electronic current appears in response to optical driving. This multitude of inter-related phenomena creates a rich, and in many aspects still open, field of study.

From the experimental and technical viewpoint this problem is no less challenging. While the above advantages of using light as a characterization and control tool in molecular electronics are obvious, application of light in molecular junctions has encountered problems stemming from the difficulty in injecting light into the narrow slit between macroscopic metal leads and from the need to discern genuine optical effects from those associated with junction heating. Heating of course is also an issue of junction stability and integrity, the attributes of molecular electronic devices that mark the line separating interesting science and viable technology.

The term "optoelectronics" is often used to discuss the study and development of electronic devices that can control, or can be controlled by, the electromagnetic field. As in the context of molecular conduction junctions we are addressing a variety of phenomena, ranging from *junction spectroscopy*, where the junction response to incident light as a tool for its

characterization is the main objective, to control – where light is used to affect the junction functionality, such as switching of or charge pumping by a molecular electronic device and to the opposite situation where a biased molecular conduction junction is acting as a light source. It should be pointed out that many of the phenomena discussed below have analogs in macroscopic and mesoscopic devices: photoconductivity and light emitting diodes are long studied subjects. Studying these phenomena in nanosystems, sometimes in single-molecule junctions, often reveals new physical origins of the observed behaviors. Tunneling induced light emission, tunneling promotion by light and Raman scattering from tunneling junctions are important examples.

Observations of light assisted electron tunneling go back half a century, when Dayem and Martin[1] reported multiphoton microwave assisted tunneling between superconductors. This observation and its interpretation by Tien and Gordon[2] still inspire the discussions of present observations. An important development was the observation of light assisted tunneling STM configurations.[3] Here, visible light (632 nm) was used to induce photoconductivity in the substrate (GaAs), thereby increasing the STM signal. Another important phenomenon, light emission from biased metal–insulator–metal junctions, was observed first by Lambe and McCarthy[4] and was realized in STM junctions by Gimzewski and coworkers.[5] The importance of the STM configuration, in addition to providing a convenient platform for the combined observation of optical and electrical signals, stems from the focusing effect of the tip that results from the electromagnetic boundary conditions (the lightening rod effect[6]) on one hand, and from the excitation (at appropriate wavelengths) of surface plasmons[7] localized at the tip–surface junction on the other. This makes it possible to conduct optical studies at sub-wavelength resolutions and provides the basis for tip-enhanced optical microscopy[8] and tip-enhanced Raman spectroscopy.[9] An early review of works on light emission in STM junctions was given by Berndt,[10] and a comprehensive state of the art review of the entire field was published a decade ago by Grafstrom.[11] In a parallel development, surface enhanced Raman scattering (SERS), more generally surface enhanced spectroscopy and photochemistry, known since the late 70s,[12–16] has evolved into a single molecule response domain,[9,17,18] making it possible to identify structures responsible for the enhancement phenomenon. The SERS enhancement was shown to be dominated by "hot spots" associated mostly with junctions and narrowly spaced intervals between small metal particles. It had been known that the electromagnetic field enhancement is particularly strong at such positions[16,19,20] and the possibility of additional enhancement associated with electron transfer between the metal particles through the Raman active molecule has been suggested.[21–23] This has led to intense studies of plasmonic properties of aggregates of metal and semiconductor particles, recently reviewed by Halas and coworkers.[24] The similar structures of molecular conduction junctions and hotspots for surface enhanced spectroscopy is what brings the fields of molecular electronics and molecular plasmonics together into what we name here molecular optoelectronics. The account given below of recent observations made on illuminated conduction junctions focuses mostly on their observed electrical

properties. However, the incident field in these works is the local field associated with the junction geometry and possibly with plasmon excitation. Indeed, in some cases surface enhancement is instrumental in obtaining a meaningful detectable signal.[25–27] In others, excitation of surface plasmons (surface plasmon resonance spectroscopy) can be used to probe structure of a molecular bridging layer through its dielectric response behavior.[28]

In what follows we provide a brief overview of the several ways by which such electromagnetic fields affect transport in molecular junctions. A perceptive reader will easily realize that, while a large body of experimental work already covers several key observations, theoretical studies have exceeded experiments in many of the aspects discussed. This partly reflects the difficulties in realizing reproducible observations of molecular optoelectronic phenomena in nanosize systems as mentioned above and, perhaps, also the fact that studies of molecular electronic transport and ultrafast spectroscopy are rarely found in one laboratory. Progress is being made on both these fronts in several laboratories, and in view of the great advantages offered by monitoring and controlling molecular conduction junctions with light, we expect this field to progress rapidly.

2. Switching

Using light to effect switching between differently conducting states of a molecular bridge is an obvious application of the combination of light and molecular conduction junctions. Conceptually the simplest idea is to effect switching by photo-induced isomerization. It is experimentally[29–31] and theoretically[31–34] established that molecular conduction properties can be highly sensitive to molecular conformations, for example the twist angle between benzene rings of biphenyl[30,31,33,34] that controls the overlap between electronic wavefunctions associated with different molecular segments. In the context of optical control of molecular junctions this was pioneered in 2003 by Dulic et al.,[35] who demonstrated one way switching, while results by He et al.[36] demonstrated reversible switching, both using photochromic dithienylethene-type molecules thiol-bonded onto gold electrodes. Using UV and visible light it is possible to switch between open and closed molecular configurations (see Fig. 1). The resistance of the open form was found to be two orders of magnitude higher than that of the closed form. Later studies have demonstrated reversible switching in different molecular systems, e.g. azobenzenes[37–40] and diarylethenes.[41–43] Theoretical calculations[44–49] were put forward to rationalize these findings and to suggest other, conceptually related, switching mechanisms.[50] It should be pointed out, however, that a most interesting theoretical problem remains open – the nature of the barrier between the two stable states associated with the switching mechanism and the dynamics of the associated barrier crossing process in the non-equilibrium, current carrying junction.[51]

An explicit change of the molecular nuclear configuration is not the only way to achieve switching. Voltage induced switching is often associated with a change in the redox state, more generally the electronic structure of the bridging molecule. This is often the case in voltage induced switching of redox molecular junctions,[53] and can be induced photochemically as well.[54–59]
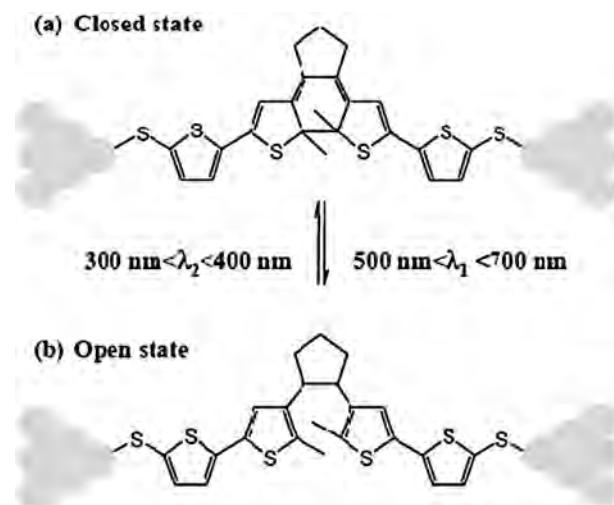
Fig. 1 (From ref. 35) Photochromic molecular switch between two Au contacts in a closed state (a) and an open state (b). By exposing the molecule to light of wavelength in the range 500 nm < λ < 700 nm, the molecule will switch from (a) to (b). In solution the protected molecule can be switched back to the (a) state by exposing it to UV light with wavelength in the range 300 nm < λ < 400 nm. However, this could not be done with the gold-connected molecules.

On the theoretical side, Wang and May[60,61] have addressed the problem of electronic switching by considering the dynamics of electronic transitions in the molecule and in the metal electrodes, in conjunction with the conduction properties of the molecular bridge in its ground and excited states, taking into account electronic–vibrational coupling and vibrational heating.

It should be noted that in many cases there is no fundamental difference between switching by photochemical conformation change and switching by affecting the electronic structure. The reason is that also in the latter case local stability is associated with accommodation of the electronic structures involved in nuclear reorganization[53,62,63] that can be substantial when the electronic states involved correspond to different molecular redox states. The dynamics of the switching process is again associated with the nuclear motion, similar to a photoinduced Marcus-type electron transfer, except that here again we need to consider such processes in electronic non-equilibrium.

Finally we note that switching by light is amenable to different implementation scenarios using different radiation wavelengths[55] and/or coherent control with appropriately shaped optical pulses.[64] For example, Thanopulos and coworkers[65,66] have proposed a porphyrin-based molecular junction that can be switched to conduct in either one of two perpendicular directions by suitably chosen optical pulse. Molecular routers have been proposed also in theoretical works by the Hänggi group[67,68] and by Peskin and Galperin.[69]

3. Effect of electromagnetic fields on junction transport

Interest in the way external radiation can affect junction transport goes back to the middle of the previous century, with the observation[1] and theoretical discussion[2] of the effect of microwave radiation on the conduction properties of

tunneling junctions. The use of microwaves[70–73] explores the adiabatic limit in which the EM field affects level oscillations but not population transfer.[74] Moreover, in this wavelength regime the effect of the field is limited to the gap between the metal electrodes, making it possible to describe the process as tunneling through a time dependent barrier. This is a problem of fundamental interest with many ramifications, exemplified by its use as a route to estimating tunneling traversal times[76] that is the time spent by electron in the classically forbidden region. More recently, visible radiation has been often used to affect electron transmission in various configurations,[55,77–82] sometimes taking advantage of tip enhanced field effects.[77,78] Inducing optical processes in scanning tunneling microscope configurations makes it possible to perform spectroscopy with an atomic scale resolution. For example, atomic resolution on a fast timescale has been achieved using a cross-polarized double-beat method where two light pulse trains are mixed by surface plasmon excitation.[83] Thus, light can be used both as a way to control junction transport and for observing molecular processes with atomic scale resolution.

Theoretical treatments of such observations and related works aimed to evaluate the influence of an external time dependent field on junction electronic transport have used a variety of methods with varying levels of sophistication. Conceptually simplest are works[84–90] that address electron transmission probabilities in the framework of scattering theory extended to account for the presence of an external electromagnetic field. While qualitative insight can be obtained from such calculations, they do not account correctly for Fermi exclusion effects that are expressed in the case of inelastic transmission.[91,92] Alternatively, several workers have used the master equation approach or similar kinetic descriptions of junction transport, again generalized to take into account the effect of an external time dependent field. Calculations involving time-periodic fields are facilitated by using Floquet's theory[68,101] (see references to other papers by the Hänggi group in these review articles), and a simplified description may be achieved by invoking the rotating wave approximation,[60,61,102–107] but general time dependence of the external field, applicable to pulse excitations, has been addressed as well[108–117] at the cost of more involved numerical work. Such an approach relies on the assumption of weak molecule–lead coupling, which may be sufficient in some situations but can miss important physical effects in others. Mathematically, a calculation of junction electronic transport to the lowest (2nd) order in the molecule–lead coupling does not account for broadening of the molecular levels due to this coupling, that is, electronic exchange between a molecule and a lead is treated as a kinetic process. The latter can be Markovian, or show non-Markovian (memory) characteristics depending on the model (wide-band or band limited) used for the lead spectral function (coupling-weighted density of states).[118] However this approach fails when the level width associated with the metal–molecule coupling ($\sim V^2 \rho$, where V is this coupling and ρ is the density of lead electronic states) is of the order of, or larger than, other energy scales that characterize the model, for example spacing between molecular levels or between molecular electronic energy and the lead Fermi energy. In such cases the transport behavior is often dominated by

mixing and interference between the broadened levels, effects that appear in higher order in the molecule–lead coupling.[119] In contrast, calculations based on the non-equilibrium Green function (NEGF) formalism[123–139] can account for such effects and provide the most general approach to this problem.

Finally we note that while much of the work cited above is based on simple free electron tight-binding junction models, some recent works combine time dependent techniques, sometimes based on the NEGF formalism, in conjunction with electronic structure calculations.[131–133,137,140–145] Other works have taken into account electron–phonon interactions, addressing the signature of such interactions in the electrical response of illuminated junctions.[60,102–104,123,124,127,128,146,147]

Arguably more important than the methodological side of our subject is the understanding that the optical response of molecular conduction junctions is underlined by several physical processes and mechanisms. Analysis of such observations should start by addressing the issue of heating of the nuclear environment, which cannot be avoided when illuminated junctions are concerned.[60,77,79,81] In what follows we will assume that this issue has been settled, either by finding conditions under which heating is negligible or by subtracting its effect out, and discuss effects of illumination on transport properties of molecular conduction junctions that arise from direct interaction of the radiation field with the electronic subsystem. The considerable theoretical literature on this subject describes several mechanisms that are manifested under suitable conditions. In addition to the plasmonic effects discussed above, such mechanisms take several forms that can be broadly cataloged as adiabatic or non-adiabatic. In the former, the driving frequency is small relative to the characteristic level spacing in the system, so that light-induced mixing between such levels can be disregarded. (As already noted, this is never true for the metal itself, however, for low frequencies the radiation filed does not penetrate into the metal environment.) In non-adiabatic processes, the driving is done with frequencies large enough to effect inter-level transitions. Within the class of adiabatic effects we can further distinguish between simple processes that can be realized under any kind of illumination, and control processes where a desired performance is achieved by suitable engineering of the external modulation. In the group of non-adiabatic processes we may distinguish between those dominated by electronic excitation of the molecular bridge and those associated with electronic excitations in the metal leads, and we may further consider non-adiabatic control. Of course, some of the processes described below may coexist, and sometimes interfere, see *e.g.* ref. 86. Some of the most commonly discussed mechanisms are outlined below.

3A. Adiabatic processes

In the low frequency limit, electronic excitations may be disregarded (we emphasize again that for a molecule interacting with the continuous spectrum of metal electrons this is never exactly correct) and the effect of an external time dependent perturbation enters through modulation of the electronic energies. Such processes take place under microwave radiation but could be equivalently realized by mechanical perturbation, *e.g.*, acoustic waves.[148,149]

Adiabatic photo-assisted tunneling. The basic mechanism of this effect has been described by Tien and Gordon.[2] The Hamiltonian is given by $\hat{H}_0 \rightarrow \hat{H} = \hat{H}_0 + eW\cos\omega t$, and in the adiabatic limit an eigenstate of $\hat{H}_0$ becomes $\Psi_0(r,t) = \psi(r)e^{-i(E/\hbar)t} \rightarrow \Psi(r,t) = \psi(r)\exp\left[-(i/\hbar)\left(Et + \int_0^t eW\cos(\omega t')dt'\right)\right] = \psi(r)e^{-i(E/\hbar)t}\sum_{n=-\infty}^{\infty} J_n(\alpha)e^{-in\omega t}$, where $\alpha = eW/\hbar\omega$, J_n is the n-th order Bessel function of the first kind and e is the electron charge. Accordingly, the density of states available for the transmitting electron becomes $\rho(E) \rightarrow \sum_{n=-\infty}^{\infty} \rho(E + n\hbar\omega)J_n^2(\alpha)$, reflecting the fact that an electron incident with energy E may end up in any replica of the original spectrum that differs from it by the energy of n absorbed or emitted photons. Using the Bardeen formalism[150] this leads to the tunneling current in the form

$$I = c\sum_{n=-\infty}^{\infty} J_n^2(\alpha) \int_{-\infty}^{\infty} dE(f_L(E) - f_R(E + n\hbar\omega))\rho_L(E)\rho_R(E + n\hbar\omega) \tag{1}$$

where c is a constant, f is the Fermi distribution and L and R refer to the left and right leads. A more general treatment of the same problem yields (*cf.* eqn (43) of ref. 151), written in the wide band approximation,[152]

$$I = 2\sum_{l=-\infty}^{\infty} \int_{-\infty}^{\infty} \frac{dE}{2\pi} \left| \sum_{k=-\infty}^{\infty} \frac{J_{-k}(\alpha)J_{k-l}(\alpha)}{E - \varepsilon_0 + (l-k)\omega + i\Gamma/2} \right|^2$$
$$\times \Gamma_L\Gamma_R[f_L(E)(1 - f_R(E + l\omega)) - f_R(E)(1 - f_L(E + l\omega))] \tag{2}$$

Note that while the qualitative implications of eqn (1) and (2) are the same, they differ in a significant way: eqn (2) takes into account interference between the different transport channels while eqn (1) does not. To highlight this difference consider for simplicity the case where the spectra of the left and right leads are flat, that is, $\rho_K(E) = \rho_K(K = L, R)$, independent of E, while in correspondence the denominator $E - \varepsilon_0 + (l-k)\omega + i\Gamma/2$ in eqn (2) is assumed to be dominated by the constant Γ term for all relevant l and k. In this case eqn (1) leads to

$$I \sim \rho_L\rho_R \sum_{n=-\infty}^{\infty} J_n^2(\alpha) \int_{-\infty}^{\infty} dE(f_L(E) - f_R(E + n\hbar\omega)) \tag{3}$$

while eqn (2) becomes (using $\Gamma \sim \rho$)

$$I \sim \rho_L\rho_R \sum_{l=-\infty}^{\infty} \int_{-\infty}^{\infty} dE \left| \sum_k J_{-k}(\alpha)J_{k-l}(\alpha) \right|^2$$
$$\times [f_L(E)(1 - f_R(E + l\omega)) - f_R(E)(1 - f_L(E + l\omega))] \tag{4}$$

Using $\sum_{k=-\infty}^{\infty} J_{-k}(\alpha)J_{k-l}(\alpha) = J_l(2\alpha)$ (*cf.* eqn (8.537) of Gradshteyn and Ryzhik[153]) and $J_l(2\alpha) = (-1)^l J_{-l}(2\alpha)$ it can be easily shown that eqn (4) can be recast into the form

$$I \sim \rho_L\rho_R \sum_{l=-\infty}^{\infty} |J_l(2\alpha)|^2 \int_{-\infty}^{\infty} dE[f_L(E) - f_R(E + l\omega)] \tag{5}$$

which is identical to eqn (3) except the additional factor of 2 in the argument of the Bessel function. We are not aware of any available experiments that can show the difference between the two results but their conceptual difference is obviously of interest.

Adiabatic rectification in asymmetric junctions. Current rectification in asymmetric molecular junctions has been widely discussed and demonstrated (see for example ref. 154–156), indeed its prediction[157] has been often marked as the starting point of the field of molecular electronics. Such junctions, when subjected to an oscillating bias potential as may be imposed by suitably polarized microwave radiation, will show an average DC current even in the absence of DC bias. To see this, write the bias potential in the form $V = V_0 + V_1\cos(\omega t)$ and expand the ensuing current in powers of V_1

$$I = I(V_0) + \frac{\partial I}{\partial V}\bigg|_{V_0} V_1\cos(\omega t) + \frac{1}{2}\frac{\partial^2 I}{\partial V^2}\bigg|_{V_0} V_1^2\cos^2(\omega t) + \ldots$$
$$= I(V_0) + \frac{1}{4}\frac{\partial^2 I}{\partial V^2}\bigg|_{V_0} V_1^2 + \frac{\partial I}{\partial V}\bigg|_{V_0} V_1\cos(\omega t)$$
$$+ \frac{1}{4}\frac{\partial^2 I}{\partial V^2}\bigg|_{V_0} V_1^2\cos(2\omega t) + \ldots \tag{6}$$

The AC voltage is seen to make a DC contribution that is determined by the voltage dependence of the differential conductance $\partial I/\partial V$. When $V_0 = 0$, $\partial^2 I/\partial V^2 \neq 0$ only for rectifying asymmetric junctions (for symmetric junctions I is an odd function of V). Another important characteristic of this phenomenon is the dependence of the rectified current on the square of the AC bias potential. This rectification mechanism has been observed experimentally,[73] and has been recently used[158,159] to estimate the local electromagnetic field intensity in the illuminated conduction junction.

Adiabatic control. Both electron pumping and suppression of electron transmission may be induced by low frequency driving of electron transport junctions. Pumping can be achieved by using two driving AC potentials of the same frequency and a suitably matched phase relationship, distorting the potential landscape at different locations in the junction.[160–162] Alternatively, applying uniform AC potentials of frequencies ω and 2ω (more generally $n\omega$ and $m\omega$, where n and m are integers of different parities[163]) to particle(s) moving in a static anharmonic potential can result in a net DC field across the system.[147,163–165] In fact, a purely harmonic bias modulation is sufficient to generate DC current in a junction with asymmetric level structure.[120,121] A general discussion of such pumping effects and their relation to classical and quantum ratchets is provided in ref. 68. On the other hand, barrier modulation can lead to current suppression when conditions for coherent destruction of tunneling are satisfied, where the optical modulation effects renormalization that suppresses the tunneling matrix element between neighboring sites on the bridge.[68,114,115]

This journal is © the Owner Societies 2012

Phys. Chem. Chem. Phys., 2012, **14**, 9421–9438 | 9425

3B. Non-adiabatic processes

When the density of accessible states or when the modulation frequency increases, non-adiabatic processes set in.[166–168] In the context of molecular conduction junctions we consider situations where the pumping frequency is in resonance with molecular electronic transitions that promote electrons from populated molecular levels below the electrode(s) Fermi energy to unpopulated levels above it. Under bias voltage this leads to larger current by increasing carrier density in much the same way as macroscopic photoconductors, except that the ensuing transport takes place in a nanojunction and may be dominated by coherent dynamics.[68,84,85,88,89,107,116,126,131,135,136,138,139,143,169–171]

At the light frequencies used in such experiments surface plasmons may be excited,[83] emphasizing again the need to consider the local electromagnetic fields in such calculations.[107,138,139,172]

Models. The main effects associated with resonance excitation of the molecular bridge component of molecular conduction junctions can be discussed in terms of simple generic models. It is important to note that in such processes, during which excited molecular states become populated, energy transfer to the metal electrodes, an efficient damping mechanism for molecular excitations at metal surfaces,[173] should be taken into account.[174] Furthermore, at resonance excitations electron–vibration interaction plays an important role. To account for these interactions we[135,136] have used, as a minimal junction model (Fig. 2) for resonance optical effects in molecular conduction junctions, a two electronic level (ground and excited states or, in a single electron orbitals representation, HOMO and LUMO) molecule coupled to the metal electrodes by standard electron exchange terms and to the radiation field by dipole coupling that promotes photon induced electron transfer between the two molecular states. The coupling associated with molecule–metal energy exchange describes electron transition between the molecular levels and the creation or annihilation of an electron–hole pair in the metal. The vibrational environment (hence referred to as 'phonons') is assumed to be harmonic with a standard polaronic electron–phonon coupling. The corresponding Hamiltonian takes the
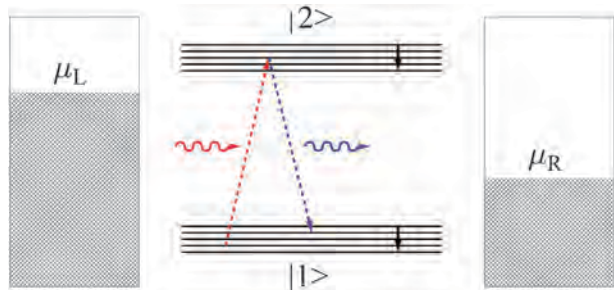
Fig. 2 A minimal model for resonant interaction of light with a molecular junction. The molecule is represented by two manifolds of vibronic states associated with the ground and excited states. The metals are represented by the boxes that represent manifolds of filled (grey)/vacant (blank) states on left and right. The incoming and outgoing photons are represented by the wavy horizontal arrows, the optical transitions are shown as dashed arrows and thermal relaxation in the two electronic manifolds is represented by dark arrows.

form (from here onwards we use $\hbar = 1$ unless an explicit note of the Planck constant is needed for clarity)

$$\hat{H} = \hat{H}_0 + \hat{V}^{(e-v)} + \hat{V}^{(et)} + \hat{V}^{(v-b)} + \hat{V}^{(e-h)} + \hat{V}^{(e-p)} \tag{7}$$

where

$$\hat{H}_0 = \sum_{m=1,2} \varepsilon_m \hat{d}_m^\dagger \hat{d}_m + \omega_v \hat{b}_v^\dagger \hat{b}_v + \sum_{k \in L,R} \varepsilon_k \hat{c}_k^\dagger \hat{c}_k + \sum_\beta \omega_\beta \hat{b}_\beta^\dagger \hat{b}_\beta + \sum_{\alpha \in \{i,\{f\}\}} \nu_\alpha \hat{a}_\alpha^\dagger \hat{a}_\alpha \tag{8}$$

includes additively the independent electronic, vibrational and photon degrees of freedom, while

$$\hat{V}^{(et)} = \sum_{K=L,R} \sum_{k \in K; m} (V_{km}^{(et)} \hat{c}_k^\dagger \hat{d}_m + V_{mk}^{(et)} \hat{d}_m^\dagger \hat{c}_k) \tag{9a}$$

$$\hat{V}^{(e-v)} = \sum_{m=1,2} V_m^{(e-v)} \hat{Q}_v \hat{d}_m^\dagger \hat{d}_m \tag{9b}$$

$$\hat{V}^{(v-b)} = \sum_\beta U_\beta^{(v-b)} \hat{Q}_v \hat{Q}_\beta \tag{9c}$$

$$\hat{V}^{(e-h)} = \sum_{k_1 \neq k_2} (V_{k_1 k_2}^{(e-h)} \hat{D}^\dagger \hat{c}_{k_1}^\dagger \hat{c}_{k_2} + V_{k_2 k_1}^{(e-h)} \hat{c}_{k_2}^\dagger \hat{c}_{k_1} \hat{D}) \tag{9d}$$

$$\hat{V}_M^{(e-p)} = \sum_{\alpha \in \{i,\{f\}\}} (U_\alpha^{(e-p)} \hat{D}^\dagger \hat{a}_\alpha + U_\alpha^{*(e-p)} \hat{a}_\alpha^\dagger \hat{D}) \tag{9e}$$

describe interactions between them. Here (et) denotes the coupling associated with electron transfer between molecule and leads, (e–v) denotes the interaction between the tunneling electron and the molecular vibration, (v–b) is the coupling between the molecular vibration and the (harmonic) thermal bath, (e–h) stands for energy transfer interaction between the molecular excitation and electron–hole excitations in the leads and (e–p) denotes the coupling of such molecular excitation to the radiation field. $\hat{d}_m^\dagger(\hat{d}_m)$ and $\hat{c}_k^\dagger(\hat{c}_k)$ create (annihilate) an electron in the molecular state m and in the lead state k of energies ε_m and ε_k, respectively. $\hat{b}_\nu^\dagger(\hat{b}_\nu)$ and $\hat{b}_\beta^\dagger(\hat{b}_\beta)$ create (annihilate) vibrational quanta in the molecular mode ν and the thermal bath mode, β, respectively. ω and ν denote frequencies of phonon modes and of the radiation field (photon) modes, respectively. Also

$$\hat{Q}_j \equiv \hat{b}_j + \hat{b}_j^\dagger \quad j = \nu, \beta \tag{10}$$

are displacement operators for the molecular (ν) and thermal bath (β) vibrations, respectively, and

$$\hat{D} = \hat{d}_1^\dagger \hat{d}_2; \quad \hat{D}^\dagger = \hat{d}_2^\dagger \hat{d}_1, \tag{11}$$

sometimes referred to as molecular polarization operators, are annihilation and creation operators for the molecular excitation. Finally, $\hat{a}_\alpha^\dagger(\hat{a}_\alpha)$ stands for creation (annihilation) operators of the radiation field quanta while i and f in eqn (8) correspond to the incident (pumping) radiation field mode and to the outgoing modes, respectively. Note that the molecule–radiation field coupling, eqn (9e), is written in the rotating

9426 | Phys. Chem. Chem. Phys., 2012, **14**, 9421–9438

This journal is © the Owner Societies 2012

wave approximation (RWA), limiting this description to the case of weak near resonant incident field.

In this model, non-equilibrium boundary conditions are effected through suitable assumptions about the states of external environments. The left (L) and right (R) metal leads are assumed to be in their own thermal equilibria characterized by the ambient temperature T and the electronic chemical potentials μ_L and μ_R whose difference $\mu_L - \mu_R = e\Phi$ corresponds to the bias potential Φ. The external thermal bath is represented by the boson modes β that are assumed to be at the ambient temperature. The radiation field is another boson environment which, in the application considered below, is taken to comprise one mode populated by 1 photon (the pumping mode) with all other modes unpopulated. For the linear optical processes discussed below this yields the photon flux per incident photon.

An important technical step, often applied in analysis of molecular vibronic spectra, is the use of canonical (small polaron or Lang–Firsov) transformation[176–178] to eliminate electron–molecular vibration coupling (for detailed discussion see ref. 179), leading to a transformed Hamiltonian of the same form as eqn (7)–(9), in which the electron creation (annihilation) operators in the molecular subspace become dressed by molecular vibration shift operators $\hat{X}_m$

$$\hat{X}_m \equiv \exp[i\lambda_m \hat{P}_v] \quad \lambda_m \equiv \frac{V_m^{(e-v)}}{\omega_v} \quad (m = 1, 2) \quad (12)$$

where $\hat{P}_\nu \equiv -i(\hat{b}_\nu - \hat{b}_\nu^\dagger)$ so that

$$\hat{d}_m \rightarrow \hat{d}_m \hat{X}_m, \quad m = 1,2 \quad (13)$$

$$\hat{D} \rightarrow \hat{D}\hat{X} \quad (14)$$

$$\hat{X} \equiv \hat{X}_1^\dagger \hat{X}_2 = \exp[i(\lambda_2 - \lambda_1)\hat{P}_v] \equiv \exp[i\lambda \hat{P}_v] \quad (15)$$

This transformation also shifts the molecular electronic orbital energies (polaronic shift) according to

$$\bar{\varepsilon}_m = \varepsilon_m - \lambda_m V_m^{(e-v)} \quad (m = 1,2) \quad (16)$$

Below we assume that this shift is taken into account and will drop the bar above ε_m.

The model (7)–(9) is useful for describing steady state situations encountered under CW optical pumping or when light emission is observed in biased junction (as discussed below). A variant of this model is convenient for discussing electrical response that results from transient (pulse) pumping. In this case it is more convenient to treat the incident pulse classically, while maintaining the quantum description for the outgoing photon fluxes.[180] In this case the last term in eqn (8) becomes $\sum_{\alpha \in \{f\}} \nu_\alpha \hat{a}_\alpha^\dagger \hat{a}_\alpha$ and eqn (9e) is replaced by

$$\hat{V}_M^{(e-p)} = \sum_{\alpha \in \{f\}} (U_\alpha^{(e-p)} \hat{D}^\dagger \hat{a}_\alpha + U_\alpha^{*(e-p)} \hat{a}_\alpha^\dagger \hat{D})$$
$$- (1/2)(\boldsymbol{e} \cdot \boldsymbol{d})\{\hat{D}^\dagger \varepsilon(t) \exp[-i\nu_i t + i\Phi(t)] + hc\} \quad (17)$$

where $\boldsymbol{e}$ and $\boldsymbol{d}$ are, respectively, the incident field polarization vector and the molecular dipole matrix elements between levels 1 and 2, ν_i is now the carrier frequency of the incoming

field (pumping frequency) and $\varepsilon(t)$ is the pulse envelope function (assumed to vary on a timescale slow relative to ν_i^{-1}) and $\Phi(t)$ is the (potentially time dependent) phase of the incoming field. Note that, unlike eqn (9e), the rotating wave approximation is not employed in eqn (17) for the system–incident pulse interaction, so it can be used to study the junction response to off-resonance strong incident pulses. Also below we discuss the use of a chirped incident pulse where $\Phi(t) = (1/2)\phi t^2$ represents a pulse whose carrier frequency changes linearly with time at the rate ϕ.

In the evaluation of physical observables using the model Hamiltonian (7)–(9), the Hamiltonian coupling parameters are translated to physical rates and energy shifts. Of particular relevance are the rates of electron transfer from molecular levels $m = 1,2$ to the electrodes $K = L, R$,

$$\Gamma_{Km} = 2\pi \sum_{k \in K} \left| V_{km}^{(et)} \right|^2 \delta(\varepsilon_m - \varepsilon_k) = 2\pi \overline{\left(\left| V_{km}^{(et)} \right|^2 \rho_K \right)}_{\varepsilon_k = \varepsilon_m}, \quad (18)$$

where ρ_K is the density of states in the manifold of single electron states of the electrode K and the average is over all states of the indicated energy, and the rate of energy transfer from the excited molecule to electron–holes excitations in the metals is given by

$$B_K(\varepsilon_{21}, \mu_K) = \int \frac{dE}{2\pi} C_K(E, \varepsilon_{21}) f_K(E)[1 - f_K(E + \varepsilon_{21})]; \quad K = L, R \quad (19)$$

where

$$C_K(E, \varepsilon) = (2\pi)^2 \sum_{k,k' \in K} \left| V_{k,k'}^{(e-h)} \right|^2 \delta(E - \varepsilon_k)\delta(E + \varepsilon - \varepsilon_{k'}) \quad (20)$$

and where $f_K(E)$ is the Fermi function of the lead K, μ_K is the corresponding electrochemical potential and $\varepsilon_{21} = \varepsilon_2 - \varepsilon_1$ is the molecular energy gap. Other important parameters are the radiative decay, γ_P, and, when electron–vibration coupling is considered, the thermal relaxation rate,

$$\gamma_v = 2\pi \sum_\beta \left| U_\beta^{(v-b)} \right|^2 \delta(\omega_v - \omega_\beta).$$

Absorption and light induced current. Using the model (9), the response of the system to weak, near resonance incident electromagnetic field can be evaluated by considering the ensuing electronic currents that can be calculated using the Keldysh nonequilibrium Green's function (NEGF) formalism. The steady state flux associated with a particular process B is obtained from the system Green's functions and the associated self-energies by[181]

$$I_B = \int_{-\infty}^{+\infty} \frac{dE}{2\pi} \text{Tr}[\Sigma_B^<(E)G^>(E) - \Sigma_B^>(E)G^<(E)] \quad (21)$$

where $G^<(E)$ and $G^>(E)$ are the lesser and greater projections of the single-electron Green function that characterize, respectively, the electron and hole populations in the non-equilibrium molecular system, while $\Sigma_B^<(E)$ and $\Sigma_B^>(E)$ are the lesser and greater projections of the electron self-energies,

characterizing the in- and out-scattering of electrons into states at energy E caused by the process B.

Eqn (21) gives the net current as the difference between in- and out-scattering fluxes, and the trace indicates a sum over all contributions to the corresponding fluxes. It should be properly adapted for use in particular applications. For example, the absorption flux can be obtained as the flux from level 1 to level 2 (see Fig. 2), given by[182,183]
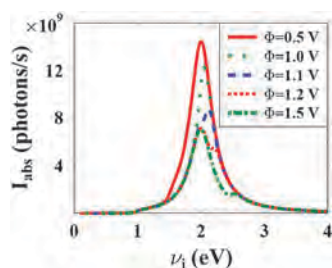
$$I_{abs}(\nu_i) = \int_{-\infty}^{\infty} \frac{dE}{2\pi} [\Sigma_{i,22}^{(P)<}(E)G_{22}^{>}(E) - \Sigma_{i,22}^{(P)>}(E)G_{22}^{<}(E)]$$

$$= -\int_{-\infty}^{\infty} \frac{dE}{2\pi} [\Sigma_{i,11}^{(P)<}(E)G_{11}^{>}(E) - \Sigma_{i,11}^{(P)>}(E)G_{11}^{<}(E)]$$

(22)

where $\Sigma_i^{(P)}$ is the self-energy associated with the incident mode part of the interaction (9e) (eqn (29) of ref. 136) and where the signs correspond to flux direction from molecular state 1 to molecular state 2 (in fact, this is a calculation of the flux from the state 1-with-one-photon to that of state 2-without-photons). The resulting absorption profile for a purely 2 level molecule (no vibrations and no electron–phonon coupling) is shown in Fig. 3.[135,136] In the unbiased junction and at low bias, when both chemical potentials are within the HOMO–LUMO gap of the molecule, the absorption spectrum is a Lorentzian characterized by the width associated with the molecule–metal coupling. In the present idealized model this width is given by $\Gamma = \sum_{K=L,R} \sum_{m=1,2} \Gamma_{Km}$ where Γ_{Km} is given by eqn (18). In reality, other dissipation processes may contribute to this width, however the metal induced damping is often dominant. The deviation from Lorentzian shape seen at higher biases reflects the partial populations formed in the molecular HOMO and LUMO due to electron transfer to/from the leads.

It should be emphasized that this calculation does not consider an additional voltage dependent effect: the Stark shift associated with the electric field in the biased cavity. Note also that such a lineshape is not readily observable, although, in principle, it could be monitored indirectly by its effect on the junction transport behavior.[184]

To calculate the effect of illumination on the junction current, eqn (21) is employed again, now with the process B identified with molecule–lead electron transfer. Formally, the
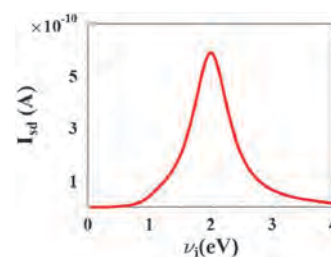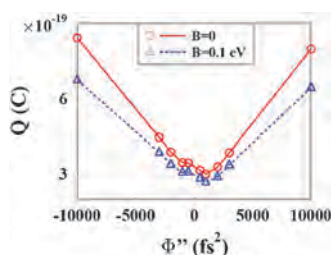

Fig. 4 (From ref. 136) Photocurrent in a light-driven junction plotted against the driving frequency for the junction parameters $\Gamma_{L,1} = \Gamma_{R,1} = 0.2$ eV; $\Gamma_{L,2} = 0.02$ eV; and $\Gamma_{R,2} = 0.3$ eV. Other parameters are as in Fig. 3.

resulting expression is the same as the standard expression for the current given by the Meir and Wingreen extension of the Landauer formula,[185] except that the molecular Green functions should be calculated in the presence of the interaction (9e). Of particular interest is the possibility to induce photocurrent in the unbiased junction. Intuitively, this can be expected in junctions where the molecular HOMO is coupled more strongly to one electrode while the LUMO is coupled more strongly to the other. In ref. 135 and 136 we have suggested that this may be achieved with molecular bridges that show a strong charge transfer transition in the direction that connects the two leads. Such charge-transfer properties can lead to the desired asymmetric coupling behaviour of the bridge, and provide an internal driving force in the illuminated junction that would result in photovoltage in the corresponding open circuit and should lead to current in the connected junction. Fig. 4 shows the current computed from the model (7)–(9) (without vibrations) under such conditions. The photocurrent peaks at the resonance frequency, $\nu_i = \varepsilon_{21}$, and the width is determined by the molecule–leads coupling.

To end this discussion, we note that while the enhancement of current under illumination is easily appreciated, light can also lead to current suppression under certain bias and coupling conditions. Such an example was recently demonstrated in ref. 138.

Non-adiabatic control. Coherent optical control in many level systems has been explored in different contexts.[186] Tailoring a pulse structure as a way to optimize its effect on the performance of molecular conduction junctions has been studied by Kleinekathöfer and coworkers[112] within a master equation methodology. A similar methodology was used by Fainberg et al.,[116] who using the semiclassical analog of the model (7)–(9) (with eqn (9e) replaced by (17)) have generalized the work in ref. 135 and 136 to the case of strong incident light pulse and, furthermore, examined the effect of using a chirped pulse to enhance the light induced current effect by the adiabatic rapid passage mechanism.[187,188] The effect of pulse chirping in this case is to induce crossing as a function of time of the energies that correspond to the excited state and to the photon-dressed ground state. In this case, transition between the two states is affected with probability 1 in the adiabatic limit of the corresponding Landau–Zener process. This work, valid only for weak molecule–metal coupling, was extended by Fainberg et al.[139] in two ways. First, using the time dependent

Fig. 3 (From ref. 136) Absorption spectrum in a junction for several bias potentials Φ. The chosen model parameters correspond to the electron and energy transfer rates $\Gamma_{L,1} = \Gamma_{R,1} = 0.01$ eV, $\Gamma_{L,2} = \Gamma_{R,2} = 0.2$ eV, $B_L = B_R = 0.1$ eV and a molecular radiative decay rate $\gamma_P = 10^{-6}$ eV. The molecular energy gap is $\varepsilon_{21} = 2$ eV.

Fig. 5 (Reproduced from ref. 139) Charge pumped by a given pulse plotted against the pulse chirp rate for an unbiased junction with $\Gamma_{L,1} = \Gamma_{R,2} = 0.1$ eV and $\Gamma_{L,2} = \Gamma_{R,1} = 0.01$ eV and $B = 0.1$ eV (blue dashed line with triangles), $B = 0$ (red solid line with circles). Other parameters are taken as in Fig. 3. For details concerning the chirped pulse see ref. 139.

NEGF formalism of ref. 125, the full effect of hybridization of the molecular and metal electronic levels could be considered. Second, the time dependent local field, that reflects the instantaneous plasmonic response of the junction structure to the incident chirped pulse, was taken explicitly into account by solving the time dependent Maxwell equations using the finite difference time domain (FDTD) approach.[189] The results of this calculation, for a particular given junction shape, are shown in Fig. 5. A considerable effect of the chirp is seen. The slight asymmetry between positive and negative chirps reflects the frequency dependent plasmonic response of the metal structure.

Another control mechanism, studied by several workers, explores the dynamics of Rabi oscillations in the illuminated bridging system.[69,126,190,191] In its simplest conceptual form that can be demonstrated by the two state junction model[126] (Fig. 2 without the vibrational substructure), improving performance by Rabi dynamics is conceptually similar to using a π pulse to optimize population transfer from ground to exited state in the isolated bridge. Such processes have been studied at different levels of theory: an early treatment using scattering theory is described in ref. 192. A more recent treatment[191] is based on the master equation approach. Ref. 126 is based on the time dependent NEGF formalism of ref. 125. An experimental observation of this phenomenon is described in ref. 193.

More complex schemes, where Rabi oscillations generated on one 2-level bridge site control the effective coupling to another were described in ref. 69 and 194 (see ref. 190 for the corresponding treatment of the isolated bridge). Such schemes can be used not only to optimize charge pumping, but also, when several pathways are involved, to effect coherent controlled switching between them.[69]

Electronic excitation of the leads. While most of the theoretical treatments reviewed above focus on optical excitation of the molecular bridge, it is clear that optical excitation of the leads cannot be realistically disregarded. The effect of illumination on the current observed between a metal tip and a semiconductor surface is most readily interpreted by generation of optically excited electrons and holes (see ref. 11 and references therein). Observations of light induced current in STM junctions involving absorbed molecules[78,80] have been interpreted in a similar way. To generalize the models (7)–(9) and (17) to include such effects, two additional interaction terms should be included: in addition to excitation of

electron–hole pairs in the metals, light may also induce electron transfer between molecule and metals. Formally, such interaction terms take the forms

$$\hat{V}_{CT}^{(e-p)} = \sum_{\alpha \in \{i,\{f\}\}} \sum_{k \in \{L,R\}} \sum_{m=1,2} [V_{km,\alpha}^{(e-p)} \hat{D}_{km} + V_{mk,\alpha}^{(e-p)} \hat{D}_{mk}](\hat{a}_\alpha + \hat{a}_\alpha^\dagger)$$

(23)

$$\hat{V}_{eh}^{(e-p)} = \sum_{\alpha \in \{i,\{f\}\}} \sum_{k,k' \in \{L,R\}} \sum_{m=1,2} [V_{kk',\alpha}^{(e-p)} \hat{D}_{kk'} + V_{k'k,\alpha}^{(e-p)} \hat{D}_{k'k}](\hat{a}_\alpha + \hat{a}_\alpha^\dagger)$$

(24)

where

$$\hat{D}_{mk} \equiv \hat{d}_m^\dagger \hat{c}_k; \hat{D}_{km} \equiv \hat{c}_k^\dagger \hat{d}_m \text{ and } \hat{D}_{k'k} \equiv \hat{c}_{k'}^\dagger \hat{c}_k$$

(25)

In the alternative description analogous to the model (17), the terms $(\hat{a}_\alpha + \hat{a}_\alpha^\dagger)$ associated with the incoming mode $\alpha = i$ are replaced by classical time dependent fields. Note that the polaron transformation described by eqn (12)–(15) also renders $\hat{D}_{mk} \rightarrow \hat{D}_{mk} \hat{X}_m^\dagger$; $\hat{D}_{km} \rightarrow \hat{D}_{km} \hat{X}_m$.

Actual calculations in models that involve the interactions (23) and (24) are quite involved, see for example ref. 195 and 196. Indeed the few theoretical descriptions of the manifestation of such electron transfer processes have so far relied on simple kinetic description of these processes.[60]

## 4. Light emission from current carrying junctions

Light emission from tunneling junction has been known for a long time. Many observations are consistent with a picture of light emitted by junction plasmons that are excited by the tunneling electrons as the source of the observed emission.[4,10,197–208] This interpretation is supported by a substantial body of theoretical work.[209–215] Obviously, other fluorescent modes can also be excited.[206,216,217] In particular, when a molecule, molecules or other types of quantum dots occupy the tunneling gap, emission from excited molecular states can also be observed.[218–231] It should be kept in mind that such excitations can still be coupled to the junction plasmons.[232–237] Several theoretical treatments of light emission from the molecular component of biased molecular conduction junctions were recently presented.[135,136,237–240]

Light emission from excited molecules in close proximity to a metal surface is usually a low yield process because of efficient competing non-radiative channels: energy and electron transfer to the metal. The efficiency of the latter can be made smaller by using a non-metallic conducting substrate or by separating the molecule(s) from the metal by an insulating, usually metal oxide, layer. Fig. 6 shows the first (to our knowledge) observation of such a process by Flaxer et al.,[218] while Fig. 7 demonstrates the power of this method as applied recently by Wu et al.[241] In the latter, light emission is seen to contain vibrational information (see ref. 226, 230 and 231 for similar observations) that can be probed with sub-molecular resolution.

Light emission from junction plasmons or from the molecular bridge can be pictured as resulting from excitation of the fluorescing species by the time dependent potential of the tunneling electron. Alternatively, within a non-interacting
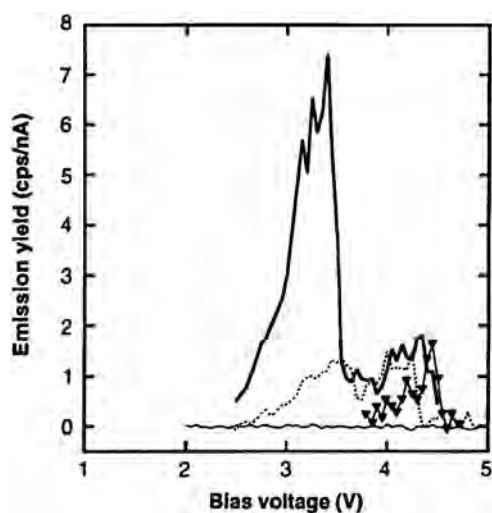
Fig. 6 (Reproduced from ref. 218) The bias voltage dependence of light emission from a squeezable tunnel junction (measured by the emission yield in counts per second (cps) per nanoampere) with DCA (9,10-dichloroanthracene)-coated ITO (Indium Tin Oxide, a transparent conductor). The full line with triangles represents the emission from bare ITO. The full and the dotted line represent the emission from a DCA-coated ITO surface at 0.5- and 0.05-layer coverage, respectively. The tunneling current is 50 nA. Practically no counts were measured for the DCA-coated metal (horizontal wavy line near zero counts). The loss of signal at high voltage results from an irreversible destruction of the junction. See ref. 218 for further details.
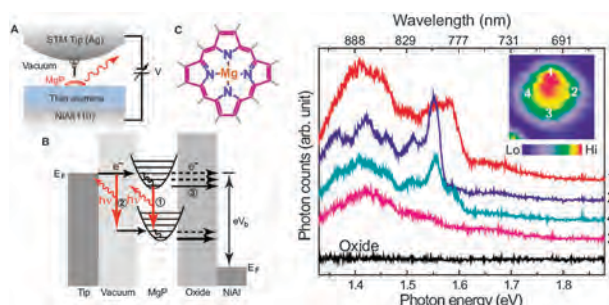
Fig. 7 (Reproduced from ref. 241) Left: a schematic sketch (A) and an energy diagram (B) of a STM junction, in which a single magnesium porphine MgP molecule (C) is adsorbed on a thin insulating alumina film grown on a NiAl(110) surface. Along with the intramolecular radiative transition (1), other pathways (2) and (3) of the tunneling electrons are marked in the diagram. Right: spatial dependence of the emission spectra from an MgP molecule adsorbed on an oxidized NiAl(110) surface. The locations of the STM tip where each spectrum was collected are marked in the STM image of this molecule (inset) (see ref. 241 for details).

electron model, the tunneling flux through the molecule can create an excess electron population in the LUMO and excess hole population in the HOMO, effectively exciting the molecule, as seen in panel C of Fig. 7. This mechanism is similar to that underlying the operation of a light emitting diode, except that it now takes place in a single molecule. As such, it can be described within the model (7)–(9), where now the flux of interest is given by an expression similar to eqn (22), except that $\Sigma_{i,mm}^{(P)}$ is replaced by $\Sigma_{mm}^{(P)}$ ($m = 1,2$) – the self-energy
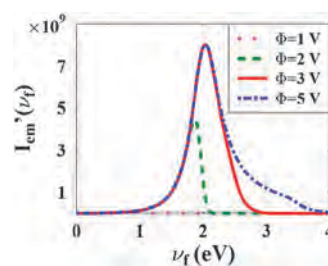
Fig. 8 (Reproduced from ref. 136): fluorescence, shown for several values of the voltage bias, in a junction comprising a 2-level molecular bridge (no vibrational structures). The parameters used are $\Gamma_{Km} = 0.1$ eV ($K = $ L,R and $m = 1,2$). Other parameters are as in Fig. 3.

associated with the coupling of the molecular 1–2 transition to the outgoing photons (eqn (38) of ref. 136). Interestingly, such calculations indicate that the emitted spectrum will depend on the bias potential (see Fig. 8) for the same reason as in Fig. 3, as the broadened molecular levels become partially populated.

To end this section, it should be noted that the theoretical treatments of light emission from tunneling junctions, whether plasmon or molecular based, suggest a bias threshold of $V = \hbar \nu_f / e$ for this process, where ν_f is the frequency of the emitted photon with maximum intensity at $\nu_f = \omega_p$ (plasmon frequency) or $\nu_f = \varepsilon_{21}$ (molecular resonance). While this agrees with most experimental observations as well as with our common view of the conceptually similar phenomenon of inelastic electron tunneling spectroscopy (where phonons replace photons as the bosonic degrees of freedom interacting with the tunneling electrons), there are some experimental indications that a non-linear process may take place as well. Thus, Berndt and coworkers[242,243] as well as Dong et al.[244,245] have observed above threshold emission, $\hbar\omega > eV$, from tunnel junctions, suggesting the possible involvement of 2-electron processes. So far there has been no full theoretical description of this phenomenon, however an attempt to describe it in terms of the non-linear effects of current fluctuations in the junction has been recently made[246] based on a theory of non-linear junction noise by Nazarov and coworkers.[247] Indeed, the close connection between current noise and light emission from tunnel junctions is intuitively expected, and has been clearly demonstrated in a recent experiment.[248]

5. Raman scattering

As noted in the Introduction, optical spectroscopy of molecular conduction junctions lies at the juncture of the two contemporary fields: molecular electronics and molecular plasmonics. Raman scattering from molecular junction is a prime example. Surface enhanced Raman scattering (SERS)[15,21,249] is mainly caused by the local enhancement of the radiation field at rough features on certain noble metal surfaces.[6,16,19,20] Recent observations of "giant" SERS[250] have been attributed to molecules positioned in special "hotspots" characterized by particularly strong electromagnetic field enhancement. Such hotspots are often identified with narrow gaps between metal particles – essentially a nanojunction.[23] In addition to the electromagnetic enhancement, SERS is affected also by first layer, "chemical" effects associated with electron

9430 | *Phys. Chem. Chem. Phys.*, 2012, **14**, 9421–9438

This journal is © the Owner Societies 2012

transfer between molecular and metal orbitals.[21,251–253] This becomes particularly significant in molecular conduction junctions whose operation reflects directly such electron transfer. It has been suggested that electron motion through the molecule in metal–molecule–metal contacts will reduce the EM field enhancement and at the same time may open a new channel for Raman scattering.[22] Such new channels may indeed be quantified[254] as outlined below. More generally, considering that inelastic electron tunneling spectroscopy is arguably the most important diagnostic tool available today for molecular conduction junctions, it should be obvious that SERS and SERRS (surface enhanced resonance Raman spectroscopy) can, in principle, provide the same type of information at potentially higher resolution and under different bias conditions. This has been the driving force for several recent efforts to introduce Raman scattering in such systems[26,255,256] that have led, perhaps not surprisingly, to the observation of correlation between the Raman signal and the onset of molecular conduction.[27] In addition to providing structural and dynamical information,[257–262] the ratio between the Stokes and anti-Stokes components of the Raman signal can be used to monitor heating in the non-equilibrium junction.[25,263,264] The *Raman temperature* can be defined by

$$T_{\text{Raman}} = \frac{\hbar\omega_v/k_{\text{B}}}{\ln\left(\frac{J_{\nu_i\to\nu_i-\omega_v}(\nu_i+\omega_v)^4}{J_{\nu_i\to\nu_i+\omega_v}(\nu_i-\omega_v)^4}\right)} \quad (26)$$

Here ν_i and ω_ν are the frequencies of the pumping mode and the molecular vibration and $J_{\nu_i\to\nu_f}$ is the energy resolved Raman flux.[265] Eqn (26) can be used as a measure for heating provided that other factors that can affect the Stokes–anti Stokes ratio have been factored out. In the present context such effects can result from the frequency dependent electromagnetic enhancement associated with the underlying surface plasmon spectrum.[268,269]

Theoretical discussion of Raman scattering from a biased molecular junction in the framework of the model (7)–(9) has been presented in ref. 195, 196, 266, 267 and 270. It is important to emphasize again that the molecule–radiation field coupling in these model calculations should reflect the properties of the *local* electromagnetic field at the molecular site as calculated in several recent publications.[107,138,139,172] In contrast to the calculation of absorption and emission described above, Raman scattering cannot be associated with an intramolecular electronic current, so a relationship analogous to eqn (22) cannot be used. Instead we note that the Raman flux is a sum over final photon modes ($\alpha \in \{f\}$) of outgoing fluxes which (to lowest order) are of 4th order in the interaction with the electromagnetic field: 2nd order in the interaction with the pumping mode and 2nd order with the final (accepting) mode. A general non-equilibrium expression for the net flux between the molecule and any photon mode α is[196]

$$J_\alpha(t) \equiv -\frac{d}{dt}\langle \hat{a}_\alpha^\dagger(t)\hat{a}_\alpha(t)\rangle$$
$$= -\int_{-\infty}^{t} dt'[\Pi_\alpha^<(t,t')\mathscr{G}^>(t',t) + \mathscr{G}^>(t,t')\Pi_\alpha^<(t',t)$$
$$- \Pi_\alpha^>(t,t')\mathscr{G}^<(t',t) - \mathscr{G}^<(t,t')\Pi_\alpha^>(t',t)]$$
$$(27)$$

(the choice of sign reflects a notation by which fluxes into the molecule are taken positive) which at the steady state (where $f(t,t') = f(t-t')$ for all functions in eqn (27)) takes the form[271]

$$J_\alpha = -\int_{-\infty}^{\infty} dt[\Pi_\alpha^<(-t)\mathscr{G}^>(t) - \Pi_\alpha^>(-t)\mathscr{G}^<(t)] \quad (28)$$

In eqn (27) and (28) $\Pi_\alpha^{>,<}$ are the greater (lesser) projection of the molecular self-energy due to coupling to the radiation field mode α,

$$\Pi_\alpha^{>,<}(t,t') = |U_\alpha^{(e-p)}|^2 F_\alpha^{>,<}(t,t') \quad (29)$$

where $F_\alpha^{>,<}$ are the greater (lesser) projections of the free photon GF in mode α, which on the Keldysh contour[272,273] takes the form

$$F_\alpha(\tau,\tau') \equiv -i\langle T_c \hat{a}_\alpha(\tau)\hat{a}_\alpha^\dagger(\tau')\rangle, \quad (30)$$

and $\mathscr{G}^{>,<}$ are the greater (lesser) projections of the molecular polarization GF (dressed by molecular vibration shift operator)

$$\mathscr{G}(\tau,\tau') \equiv -i\langle T_c \hat{D}(\tau)\hat{X}(\tau)\hat{D}^\dagger(\tau')\hat{X}^\dagger(\tau')\rangle \quad (31)$$

where the molecular operators $\hat{D}$ and $\hat{X}$ are defined in eqn (11) and (15) respectively. In (30) and (31) T_c is the time ordering operator on the Keldysh contour. Here and below we use t to indicate real time variables, while τ is reserved for time variables on the Keldysh contour. Note that, in contrast to eqn (21) where $G^{>,<}$ represents single electron Green functions, the function $\mathscr{G}(\tau,\tau')$ and its projections are two-electron Green functions – correlation functions of the phonon-dressed molecular polarization operators.

Next, consider the steady state radiative flux, eqn (28), and note that the first and second terms on the r.h.s. correspond to fluxes out of and into the mode α, respectively. Focusing on one final (accepting) mode of the photon bath, $\alpha = f$, and on the out-scattering flux into this mode

$$J_f = \int_{-\infty}^{+\infty} dt\Pi_f^>(-t)\mathscr{G}^<(t) \quad (32)$$

we see that $\Pi_f^>$ is (to lowest order) 2nd order in the coupling between the molecule and this mode. Therefore the contribution of mode f to the steady state Raman flux is obtained by expanding $\mathscr{G}^<(t)$ in the interaction with the pumping mode i, and replacing $\mathscr{G}^<(t)$ in (32) by the second order term in this expansion. This leads to the Raman flux $J_{i\to f}$ as a sum of three contributions. A "normal" term, associated with a photon scattering process where the molecule starts and ends in the ground state, is the generalization to non-equilibrium of the standard resonance Raman scattering result. An "inverse Raman" term associated with the analogous process in which the molecule starts and ends in the excited state is appreciable only when the bias is high enough so as to have populations in both the HOMO and LUMO. The third term results from interference between these pathways. Explicit forms of these contributions are provided in ref. 196.

Some generic behavior patterns resulting from this model calculation are displayed in Fig. 9. Panel (a) shows the electronic current (full line, red) and the integrated Raman signal (dashed line, blue) plotted against the bias voltage. In this two-level model the onset of electric current signifies that
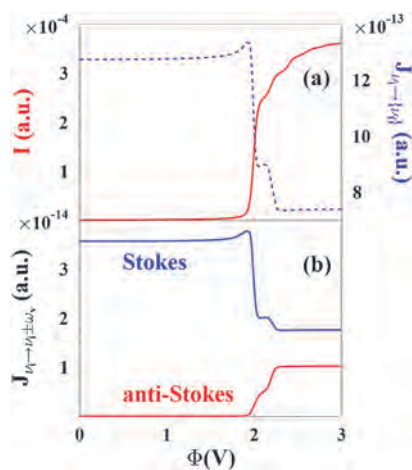
Fig. 9 (From ref. 281) The source–drain current and the total Raman flux (a) and the Stokes and anti-Stokes components of the Raman flux (b), computed from the model described in the text, plotted against the applied bias. The parameters used in the calculation are: $\Gamma_{K,m} = 0.01$ eV (K = L,R and m = 1,2), B = 0.01 eV, ω_ν = 0.1 eV, γ_ν = 0.005 eV, $V_1^{(e-v)}$ = 0.1 eV and $V_2^{(e-v)}$ = 0.1 eV. Other parameters are as in Fig. 2.

at least one of the levels becomes partially populated, which in turn reduces the optical response, in the present case the Raman scattering. However, as seen in panel (b), the anti-Stokes component of this scattering actually increases beyond the conduction threshold – a result of the excess heating experienced by the molecular bridge in this regime.

A measure of the heating experienced by the molecular bridge is given by the Raman temperature, eqn (26). In the non-equilibrium junction, identifying this measure as an actual temperature should be regarded with caution. For one thing, this measure can depend on the vibration involved in the particular Raman line considered – there is no a priori reason to expect that in the non-equilibrium junctions all vibrational modes will be heated to the same extent. More generally, different definitions of an effective temperature of non-equilibrium junctions can yield different "temperatures". In our studies, we often invoke a thermometer-like definition: a certain location or a certain mode of a non-equilibrium system is weakly coupled to an equilibrium thermal bath, and the effective temperature of the former is defined as the temperature of the equilibrium bath for which no net heat current passes between the systems.[274]
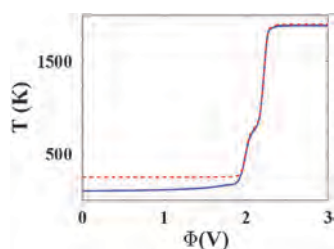
Fig. 10 (From ref. 280) The effective temperature obtained from the "thermometer definition" (full line, blue) and the Raman temperature (dashed line, red) plotted against the bias voltage. Parameters are as in Fig. 9, except that $V_2^{(e-v)}$ = 0.08 eV.

An indication that such effective temperature concepts are not entirely meaningless is seen in Fig. 10, which shows that the effective temperature defined in this way and computed for our model is not very different from the Raman temperature computed for the same model. This calculation indicates that, at least in the model considered, the effective temperature concept provides a qualitatively meaningful, even if ill-defined, extension of the equilibrium temperature to the non-equilibrium regime.[275] Still, exercising such procedures should be done with caution and with proper theoretical interpretation. A case in point is a recent measurement of the Raman
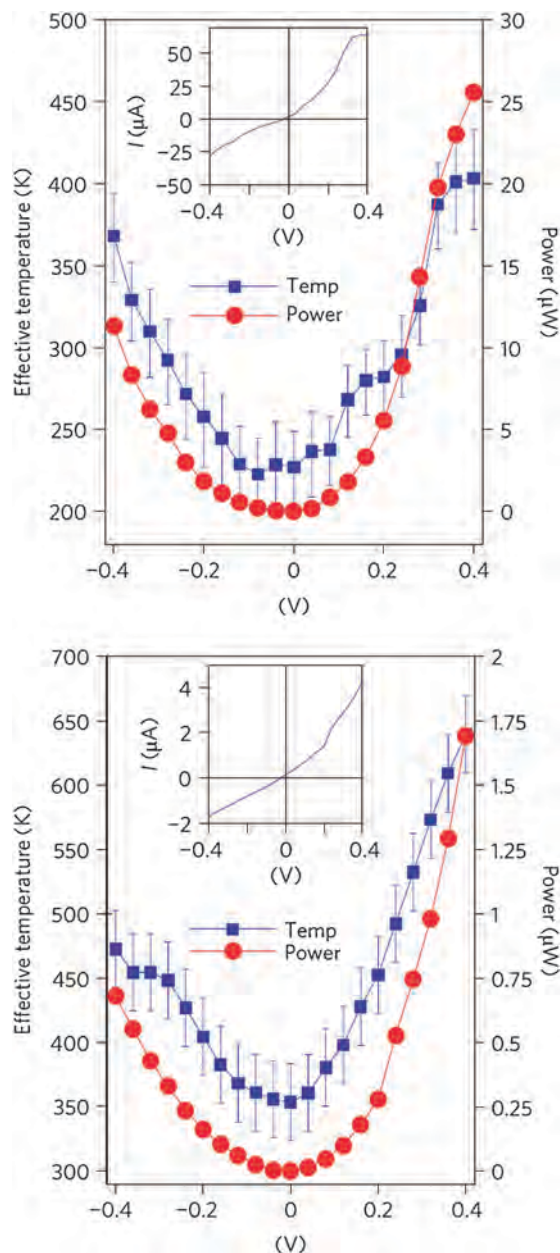
Fig. 11 (From ref. 264) The Raman temperature of the electronic background (blue squares, left axis), and the dissipated electrical power (red circles, right axis) plotted against the bias voltage in a bare junction with no molecular bridge and touching leads (upper panel) and in a junction comprising OPV3 molecules (lower panel). The insets show the corresponding current–voltage plots.

9432 | *Phys. Chem. Chem. Phys.*, 2012, **14**, 9421–9438

This journal is © the Owner Societies 2012

temperature of the electronic continuum observed in Raman scattering from junctions comprising molecular bridges and gold nanoelectrodes.[264] Fig. 11 shows the measured Raman temperature as a function of the bias voltage in a bare junction and in a junction comprising three-ring oligophenylene vinylene (OPV3) molecules between the gold leads. Note that in the presence of the molecular separator the current and the dissipated electrical power are much smaller than in the bare junction, still the temperature rise is about the same in both cases. This indicates the dominant role of the molecular bridge in inducing the observed heating. It is natural to assign, as was done in ref. 264, the observed Raman temperature to heating of the electronic distributions in the leads. However, in a recent theoretical analysis[266,267] we have found that (a) the observed effective temperature is considerably higher than an upper bound on the electronic heating in the leads, and (b) the observed heating reflects more the non-equilibrium electronic distribution in the molecular bridge than that in the metals.

As noted above, eqn (26) can be used as a measure for heating provided that other factors that can affect the Stokes–anti Stokes ratio have been factored out. In ref. 25, an observation of apparent cooling with bias has been attributed instead to the frequency dependence of the Stokes–anti Stokes ratio associated with an underlying plasmon resonance. Interestingly, theory indicates that cooling of certain vibrations may take place in voltage driven junctions[276] but, again, caution must be exercised in applying the effective temperature concept in non-equilibrium situations when trying to confirm such predictions.

Finally, consider the "chemical" or charge transfer (CT) mechanism for SERS. Many studies have attempted to characterize the role played by CT in SERS from molecules adsorbed on metal surfaces.[21,22,252,277–285] A particularly simple model by Persson[251] considers the light scattering signal resulting from the oscillating charge transfer dipole formed between an adsorbed molecule and the underline metal as evaluated within a Newns–Anderson type model.[286] The dependence of this CT dipole on the molecular vibrational coordinate gives rise to the Raman component in the scattered radiation. We have recently extended this theory to a molecule confined between the two metal electrodes of a biased molecular junction.[254] In this extension we note that the charge transfer dipole is partially suppressed by electronic screening inside the narrow confinement between metal electrodes. At the same time we have identified an additional contribution to the oscillating dipole – the dependence of the molecular permanent dipole on its charging state. The resulting chemical contribution provides an additional enhancement on top of the electromagnetic effect when resonance conditions are satisfied, namely when the photon bridges the gap between the molecular charging energy and the electrodes Fermi energies. It therefore depends, like this gap, in a predictable way on both the bias and gate potentials.

It should be kept in mind that this calculation does not address another issue, potentially important in junction configurations – the effect of charge transfer between the electrodes on the junction plasmonic response. A study of this effect within a fully quantum calculation of the optical response of a system comprising two nearly touching metal spheres has shown that electron tunneling between the spheres indeed affects their plasmon response properties.[24,287] It remains to be seen how important is this effect for the small currents usually realized in molecular conduction junctions.

6. Concluding remarks

Characterizing and controlling molecular conduction junctions with light continues to be an exciting challenge. As a theoretical problem it requires the simultaneous treatment of electrical, optical and thermal response of a system open to matter and energy and driven by both electrical bias and optical filed(s). As an experimental task it is at least as formidable: observing a meaningful signal in a system of uncertain structure and multiple response and relaxation pathways, some of which are challenging the system's physical integrity.

We note that the theoretical models used in discussing the phenomenology of optical phenomena in bias junctions are often simplified, and while making it possible to focus on the critical physical issues involved in the description of systems in both optical and electronic non-equilibrium, fall short of addressing the full complexity of systems that comprise large molecules between metal leads of unknown microscopic structure. In the treatment of such more realistic systems, it is tempting to consider simpler kinetic models based on the master equations. The model calculations based on the more rigorous NEGF approach provide benchmarks for assessing the validity of such simpler descriptions.

Despite these experimental and theoretical difficulties, this field has seen remarkable progress in the past decade, and the growing availability of scanning tip configurations that can combine optical and electrical probes suggests that further progress towards the goal of realizing molecular optoelectronics on the nanoscale is imminent. The rewards of a successful accomplishment of this goal are obvious.

Acknowledgements

References

1 A. H. Dayem and R. J. Martin, *Phys. Rev. Lett.*, 1962, **8**, 246–248.
2 P. K. Tien and J. P. Gordon, *Phys. Rev.*, 1963, **129**, 647–651.
3 G. F. A. van de Walle, H. van Kempen, P. Wyder and P. Davidsson, *Appl. Phys. Lett.*, 1987, **50**, 22–24.
4 J. Lambe and S. L. McCarthy, *Phys. Rev. Lett.*, 1976, **37**, 923–925.
5 J. K. Gimzewski, B. Reihl, J. H. Coombs and R. R. Schlittler, *Z. Phys. B: Condens. Matter*, 1988, **72**, 497–501.
6 J. Gersten and A. Nitzan, *J. Chem. Phys.*, 1980, **73**, 3023–3037.

7 D. Sarid and W. Challener, *Modern Introduction to Surface Plasmons: Theory, Mathematica Modeling, and Applications*, Cambridge University Press, Cambridge, 2010.

8 See, *e.g.* A. Neil, B. Alexandre and N. Lukas, *J. Opt. A: Pure Appl. Opt.*, 2006, **8**, S227.

9 M. D. Sonntag, J. M. Klingsporn, L. K. Garibay, J. M. Roberts, J. A. Dieringer, T. Seideman, K. A. Scheidt, L. Jensen, G. C. Schatz and R. P. Van Duyne, *J. Phys. Chem. C*, 2011, **116**, 478–483.

10 R. Berndt, *Scanning Microsc.*, 1995, **9**, 687–693.

11 S. Grafstrom, *J. Appl. Phys.*, 2002, **91**, 1717–1753.

12 M. Fleischmann, P. J. Hendra and A. J. McQuillan, *Chem. Phys. Lett.*, 1974, **26**, 163–166.

13 D. L. Jeanmaire and R. P. Van Duyne, *J. Electroanal. Chem. Interfacial Electrochem.*, 1977, **84**, 1–20.

14 M. G. Albrecht and J. A. Creighton, *J. Am. Chem. Soc.*, 1977, **99**, 5215–5217.

15 M. Moskovits, *Rev. Mod. Phys.*, 1985, **57**, 783.

16 J. I. Gersten and A. Nitzan, *Surf. Sci.*, 1985, **158**, 165–189.

17 S. Nie and S. R. Emory, *Science*, 1997, **275**, 1102–1106.

18 K. Kneipp, Y. Wang, H. Kneipp, L. T. Perelman, I. Itzkan, R. R. Dasari and M. S. Feld, *Phys. Rev. Lett.*, 1997, **78**, 1667.

19 P. K. Aravind, A. Nitzan and H. Metiu, *Surf. Sci.*, 1981, **110**, 189.

20 M. Inoue and K. Ohtaka, *J. Phys. Soc. Jpn.*, 1983, **52**, 3853.

21 A. Otto, I. Mrozek, H. Grabhorn and W. Akemann, *J. Phys.: Condens. Matter*, 1992, **4**, 1143–1212.

22 A. Otto, *Indian J. Phys., B*, 2003, **77**, 63–73.

23 L. Brus, *Acc. Chem. Res.*, 2008, **41**, 1742–1749.

24 N. J. Halas, S. Lal, W.-S. Chang, S. Link and P. Nordlander, *Chem. Rev.*, 2011, **111**, 3913–3961.

25 Z. Ioffe, T. Shamai, A. Ophir, G. Noy, I. Yutsis, K. Kfir, O. Cheshnovsky and Y. Selzer, *Nat. Nanotechnol.*, 2008, **3**, 727.

26 D. R. Ward, N. K. Grady, C. S. Levin, N. J. Halas, Y. Wu, P. Nordlander and D. Natelson, *Nano Lett.*, 2007, **7**, 1396–1400.

27 D. R. Ward, N. J. Halas, J. W. Ciszek, J. M. Tour, Y. Wu, P. Nordlander and D. Natelson, *Nano Lett.*, 2008, **8**, 919–924.

28 K. T. Shimizu, R. A. Pala, J. D. Fabbri, M. L. Brongersma and N. A. Melosh, *Nano Lett.*, 2006, **6**, 2797–2803.

29 Y. S. Park, J. R. Widawsky, M. Kamenetska, M. L. Steigerwald, M. S. Hybertsen, C. Nuckolls and L. Venkataraman, *J. Am. Chem. Soc.*, 2009, **131**, 10820–10821.

30 D. Vonlanthen, A. Mishchenko, M. Elbing, M. Neuburger, T. Wandlowski and M. Mayor, *Angew. Chem., Int. Ed.*, 2009, **48**, 8886–8890.

31 A. Mishchenko, D. Vonlanthen, V. Meded, M. Bürkle, C. Li, I. V. Pobelov, A. Bagrets, J. K. Viljas, F. Pauly, F. Evers, M. Mayor and T. Wandlowski, *Nano Lett.*, 2010, **10**, 156–163.

32 R. Gutierrez, G. Fagas, G. Cuniberti, F. Grossmann, R. Schmidt and K. Richter, *Phys. Rev. B: Condens. Matter Mater. Phys.*, 2002, **65**, 1–4.

33 G. C. Solomon, D. Q. Andrews, R. P. V. Duyne and M. A. Ratner, *ChemPhysChem*, 2009, **10**, 257–264.

34 L. H. Wang, Y. Guo, C. F. Tian, X. P. Song and B. J. Ding, *Phys. Lett. A*, 2010, **374**, 4876–4879.

35 D. Dulic, S. van der Molen, T. Kudernac, H. Jonkman, J. de Jong, T. Bowden, J. van Esch, B. Feringa and B. van Wees, *Phys. Rev. Lett.*, 2003, **91**, 207402.

36 J. He, F. Chen, P. A. Liddell, J. Andreasson, S. D. Straight, D. Gust, T. A. Moore, A. L. Moore, J. Li, O. F. Sankey and S. M. Lindsay, *Nanotechnology*, 2005, **16**, 695–702.

37 P. Ahonen, T. Laaksonen, D. J. Schiffrin and K. Kontturi, *Phys. Chem. Chem. Phys.*, 2007, **9**, 4898–4901.

38 A. S. Kumar, T. Ye, T. Takami, B.-C. Yu, A. K. Flatt, J. M. Tour and P. S. Weiss, *Nano Lett.*, 2008, **8**, 1644–1648.

39 J. M. Mativetsky, G. Pace, M. Elbing, M. A. Rampi, M. Mayor and P. Samorì, *J. Am. Chem. Soc.*, 2008, **130**, 9192–9193.

40 C. Pakula, V. Zaporojtchenko, T. Strunskus, D. Zargarani, R. Herges and F. Faupel, *Nanotechnology*, 2010, **21**, 465201.

41 T. Kudernac, S. J. van der Molen, B. J. van Wees and B. L. Feringa, *Chem. Commun.*, 2006, 3597–3599.

42 N. Katsonis, T. Kudernac, M. Walko, S. J. van der Molen, B. J. van Wees and B. L. Feringa, *Adv. Mater.*, 2006, **18**, 1397.

43 S. J. van der Molen, J. Liao, T. Kudernac, J. S. Agustsson, L. Bernard, M. Calame, B. J. van Wees, B. L. Feringa and C. Schönenberger, *NanoLett.*, 2009, **9**, 76–80.

44 J. Li, G. Speyer and O. F. Sankey, *Phys. Rev. Lett.*, 2004, **93**, 248302.

45 C. Zhang, M. H. Du, H. P. Cheng, X. G. Zhang, A. E. Roitberg and J. L. Krause, *Phys. Rev. Lett.*, 2004, **92**, 158301.

46 C. Zhang, Y. He, H. P. Cheng, Y. Q. Xue, M. A. Ratner, X. G. Zhang and P. Krstic, *Phys. Rev. B: Condens. Matter Mater. Phys.*, 2006, **73**, 125445.

47 M. Kondo, T. Tada and K. Yoshizawa, *Chem. Phys. Lett.*, 2005, **412**, 55–59.

48 M. Zhuang and M. Ernzerhof, *Phys. Rev. B: Condens. Matter Mater. Phys.*, 2005, **72**, 073104.

49 M. Zhuang and M. Ernzerhof, *J. Chem. Phys.*, 2009, **130**, 114704.

50 C. Benesch, M. F. Rode, M. Čížek, R. Härtle, O. Rubio-Pons, M. Thoss and A. L. Sobolewski, *J. Phys. Chem. C*, 2009, **113**, 10315–10318.

51 This problem was recently considered for a thermal reaction by Dzhioev and Kosov,[52] however in the rather restricted limit where the electron transmission processes are fast on the nuclear timescale.

52 A. A. Dzhioev and D. S. Kosov, *J. Chem. Phys.*, 2011, **135**, 074701–074704.

53 J. D. Zhang, A. M. Kuznetsov, I. G. Medvedev, Q. J. Chi, T. Albrecht, P. S. Jensen and J. Ulstrup, *Chem. Rev.*, 2008, **108**, 2737–2791.

54 P. Orellana and F. Claro, *Phys. Rev. Lett.*, 2003, **90**, 178302.

55 S. Yasutomi, T. Morita, Y. Imanishi and S. Kimura, *Science*, 2004, **304**, 1944–1947.

56 Y. Wakayama, K. Ogawa, T. Kubota, H. Suzuki, T. Kamikado and S. Mashiko, *Appl. Phys. Lett.*, 2004, **85**, 329–331.

57 A. K. Rath, S. Sahu and A. J. Pal, *Appl. Phys. Lett.*, 2006, **89**, 142110.

58 H. Nakanishi, K. J. M. Bishop, B. Kowalczyk, A. Nitzan, E. A. Weiss, K. V. Tretiakov, M. M. Apodaca, R. Klajn, J. F. Stoddart and B. A. Grzybowski, *Nature*, 2009, **460**, 371–375.

59 S. Battacharyya, A. Kibel, G. Kodis, P. A. Liddell, M. Gervaldo, D. Gust and S. Lindsay, *Nano Lett.*, 2011, **11**, 2709–2714.

60 L. X. Wang and V. May, *J. Phys. Chem. C*, 2010, **114**, 4179–4185.

61 L. X. Wang and V. May, *J. Electroanal. Chem.*, 2011, **660**, 320–331.

62 M. Galperin, M. A. Ratner and A. Nitzan, *Nano Lett.*, 2004, **5**, 125–130.

63 A. Migliore and A. Nitzan, *ACS Nano*, 2011, **5**, 6669–6685.

64 I. Thanopulos, P. Kral, M. Shapiro and E. Paspalakis, *J. Mod. Opt.*, 2009, **56**, 686–703.

65 I. Thanopulos and E. Paspalakis, *Phys. Rev. B: Condens. Matter Mater. Phys.*, 2007, **76**, 035317–035315.

66 I. Thanopulos, E. Paspalakis and V. Yannopapas, *Nanotechnology*, 2008, **19**, 445202.

67 J. Lehmann, S. Camalet, S. Kohler and P. Hänggi, *Chem. Phys. Lett.*, 2003, **368**, 282.

68 S. Kohler, J. Lehmann and P. Hänggi, *Phys. Rep.*, 2005, **406**, 379–443.

69 U. Peskin and M. Galperin, *J. Chem. Phys.*, 2012, **136**, 044107.

70 W. Seifert, E. Gerner, M. Stachel and K. Dransfeld, *Ultramicroscopy*, 1992, **42–44**(Part 1), 379–387.

71 L. P. Kouwenhoven, S. Jauhar, J. Orenstein, P. L. McEuen, Y. Nagamune, J. Motohisa and H. Sakaki, *Phys. Rev. Lett.*, 1994, **73**, 3443–3446.

72 T. Kwapinski, R. Taranko and E. Taranko, *Phys. Rev. B: Condens. Matter Mater. Phys.*, 2005, **72**, 125312–125316.

73 X. W. Tu, J. H. Lee and W. Ho, *J. Chem. Phys.*, 2006, **124**, 021105.

74 This limit is never strictly realized in a system involving partly filled continuous bands, but usually holds for the molecule as long as the distance between the molecular level and the metal(s) Fermi energy(ies) is not too small. A direct observation of electronic transition (spin flip) in MW enhanced conduction was recently published[75].

75 L. R. Schreiber, F. R. Braakman, T. Meunier, V. Calado, J. Danon, J. M. Taylor, W. Wegscheider and L. M. K. Vandersypen, *Nat. Commun.*, 2011, **2**, 556.

76 M. Buttiker and R. Landauer, *Phys. Rev. Lett.*, 1982, **49**, 1739–1742.

77 V. Gerstner, A. Knoll, W. Pfeiffer, A. Thon and G. Gerber, *J. Appl. Phys.*, 2000, **88**, 4851.

78 S. W. Wu, N. Ogawa and W. Ho, *Science*, 2006, **312**, 1362–1365.

9434 | *Phys. Chem. Chem. Phys.*, 2012, **14**, 9421–9438

This journal is © the Owner Societies 2012

79 D. C. Guhr, D. Rettinger, J. Boneberg, A. Erbe, P. Leiderer and E. Scheer, *Phys. Rev. Lett.*, 2007, **99**, 086801–086804.

80 S. W. Wu and W. Ho, *Phys. Rev. B: Condens. Matter Mater. Phys.*, 2010, **82**, 085444.

81 N. Ittah, G. Noy, I. Yutsis and Y. Selzer, *Nano Lett.*, 2009, **9**, 1615–1620.

82 T. Shamai and Y. Selzer, *Chem. Soc. Rev.*, 2011, **40**, 2293–2305.

83 J. Lee, S. M. Perdue, D. Whitmore and V. A. Apkarian, *J. Chem. Phys.*, 2010, **133**, 104706.

84 A. Tikhonov, R. D. Coalson and Y. Dahnovsky, *J. Chem. Phys.*, 2002, **117**, 567–580.

85 A. Tikhonov, R. D. Coalson and Y. Dahnovsky, *J. Chem. Phys.*, 2002, **116**, 10909–10920.

86 M. Moskalets and M. Buttiker, *Phys. Rev. B: Condens. Matter Mater. Phys.*, 2004, **69**, 205316.

87 M. Moskalets and M. Buttiker, *Phys. Rev. B: Condens. Matter Mater. Phys.*, 2004, **70**, 245305.

88 A. Keller, O. Atabek, M. Ratner and V. Mujica, *J. Phys. B: At., Mol. Opt. Phys.*, 2002, **35**, 4981–4988.

89 I. Urdaneta, A. Keller, O. Atabek and V. Mujica, *J. Phys. B: At., Mol. Opt. Phys.*, 2005, **38**, 3779–3794.

90 I. Urdaneta, A. Keller, O. Atabek and V. Mujica, *J. Chem. Phys.*, 2007, **127**, 154110.

91 S. Datta and M. P. Anantram, *Phys. Rev. B: Condens. Matter Mater. Phys.*, 1992, **45**, 13761–13764.

92 Related theoretical works on the effects of external radiation on molecular electron transfer in solution[93–99] are not subjected to this shortcoming since metal electrodes are not involved. Such an effect was realized experimentally,[100] although in a somewhat more involved setup than that used in the preceding theoretical models.

93 D. G. Evans, R. D. Coalson and Y. Dakhnovskii, *J. Chem. Phys.*, 1996, **104**, 2287.

94 Y. Dakhnovskii and R. D. Coalson, *J. Chem. Phys.*, 1995, **103**, 2908–2916.

95 Y. Dakhnovskii, V. Lubchenko and R. D. Coalson, *Phys. Rev. Lett.*, 1996, **77**, 2917–2920.

96 D. Evans, R. D. Coalson, H. J. Kim and Y. Dakhnovskii, *Phys. Rev. Lett.*, 1995, **75**, 3649–3652.

97 Y. Dakhnovskii, D. G. Evans, H. J. Kim and R. D. Coalson, *J. Chem. Phys.*, 1995, **103**, 5641.

98 Y. Dakhnovskii, V. Lubchenko and R. D. Coalson, *J. Chem. Phys.*, 1998, **109**, 691–703.

99 T. Mancal, U. Kleinekathöfer and V. May, *J. Chem. Phys.*, 2002, **117**, 636–646.

100 I. B. Martini, E. R. Barthel and B. J. Schwartz, *Science*, 2001, **293**, 462–465.

101 P. Hänggi, S. Kohler and J. Lehmann, in *Lect. Notes Physics: Introducing Molecular Electronics*, ed. G. Cuniberti, G. Fagas and K. Richter, Springer, Berlin, 2005, vol. 680, pp. 55–75.

102 V. May and O. Kuhn, *Phys. Rev. B: Condens. Matter Mater. Phys.*, 2008, **77**, 115439.

103 V. May and O. Kuhn, *Phys. Rev. B: Condens. Matter Mater. Phys.*, 2008, **77**, 115440.

104 V. May and O. Kühn, *Nano Lett.*, 2008, **8**, 1095–1099.

105 L. X. Wang and V. May, *Chem. Phys.*, 2010, **375**, 252–264.

106 L. Wang and V. May, *Phys. Chem. Chem. Phys.*, 2011, **13**, 8755–8768.

107 Y. Zelinskyy and V. May, *Nano Lett.*, 2011, **12**, 446–452.

108 U. Kleinekathöfer, G. Li, S. Welack and M. Schreiber, *Europhys. Lett.*, 2006, **75**, 139–145.

109 S. Welack, U. Kleinekathöfer and M. Schreiber, *J. Lumin.*, 2006, **119**, 462–467.

110 S. Welack, M. Schreiber and U. Kleinekathöfer, *J. Chem. Phys.*, 2006, **124**, 044712.

111 G. Q. Li, M. Schreiber and U. Kleinekathöfer, *Europhys. Lett.*, 2007, **79**, 27006.

112 G. Li, S. Welack, M. Schreiber and U. Kleinekathöfer, *Phys. Rev. B: Condens. Matter Mater. Phys.*, 2008, **77**.

113 G. Q. Li, U. Kleinekathöfer and M. Schreiber, *J. Lumin.*, 2008, **128**, 1078–1080.

114 G. Q. Li, M. Schreiber and U. Kleinekathöfer, *New J. Phys.*, 2008, **10**, 085005.

115 G. Q. Li, M. Schreiber and U. Kleinekathöfer, *Phys. Status Solidi B*, 2008, **245**, 2720–2724.

116 B. D. Fainberg, M. Jouravlev and A. Nitzan, *Phys. Rev. B: Condens. Matter Mater. Phys.*, 2007, **76**, 245329.

117 G. Li, B. D. Fainberg, A. Nitzan, S. Kohler and P. Hänggi, *Phys. Rev. B: Condens. Matter Mater. Phys.*, 2010, **81**, 165310.

118 More rigorously, non-Markovian effects appear when the metal induced molecular level width (which determines the relevant observation time) approaches other energy scalesin the problem, *e.g.*, the distance between the molecular level and the metal band edge or, when the molecular level is close to the metal Fermi energy, the width of the Fermi distribution.

119 Some master equations type approaches are able to overcome some or all of these shortcomings.[120–122]

120 J. Lehmann, S. Kohler, P. Hänggi and A. Nitzan, *J. Chem. Phys.*, 2002, **118**, 3283–3293.

121 J. Lehmann, S. Kohler, P. Hänggi and A. Nitzan, *Phys. Rev. Lett.*, 2002, **88**, 1–4.

122 S. Rahav and S. Mukamel, *J. Chem. Phys.*, 2010, **133**, 244106–244112.

123 A. L. Yeyati and F. Flores, *Ann. Phys.*, 1993, **505**, 126–132.

124 A. L. Yeyati and F. Flores, *J. Phys.: Condens. Matter*, 1992, **4**, 7341–7354.

125 A. P. Jauho, N. S. Wingreen and Y. Meir, *Phys. Rev. B: Condens. Matter Mater. Phys.*, 1994, **50**, 5528–5544.

126 C. A. Stafford and N. S. Wingreen, *Phys. Rev. Lett.*, 1996, **76**, 1916–1919.

127 B. Dong, H. L. Cui and X. L. Lei, *Phys. Rev. B: Condens. Matter Mater. Phys.*, 2004, **69**, 205315.

128 R. Lu and Z.-R. Liu, *J. Phys.: Condens. Matter*, 2005, **17**, 5859–5867.

129 Y. Zhu, J. Maciejko, T. Ji, H. Guo and J. Wang, *Phys. Rev. B: Condens. Matter Mater. Phys.*, 2005, **71**, 075317.

130 J. Maciejko, J. Wang and H. Guo, *Phys. Rev. B: Condens. Matter Mater. Phys.*, 2006, **74**, 085324.

131 J. K. Viljas, F. Pauly and J. C. Cuevas, *Phys. Rev. B: Condens. Matter Mater. Phys.*, 2007, **76**, 033403.

132 J. K. Viljas and J. C. Cuevas, *Phys. Rev. B: Condens. Matter Mater. Phys.*, 2007, **75**, 075406.

133 G. Stefanucci, S. Kurth, A. Rubio and E. K. U. Gross, *Phys. Rev. B: Condens. Matter Mater. Phys.*, 2008, **77**, 075339–075314.

134 D. Kienle, M. Vaidyanathan and F. Léonard, *Phys. Rev. B: Condens. Matter Mater. Phys.*, 2010, **81**, 115455.

135 M. Galperin and A. Nitzan, *Phys. Rev. Lett.*, 2005, **95**, 206802.

136 M. Galperin and A. Nitzan, *J. Chem. Phys.*, 2006, **124**, 234709.

137 M. Galperin and S. Tretiak, *J. Chem. Phys.*, 2008, **128**, 124705–124709.

138 M. Sukharev and M. Galperin, *Phys. Rev. B: Condens. Matter Mater. Phys.*, 2010, **81**, 165307.

139 B. D. Fainberg, M. Sukharev, T. H. Park and M. Galperin, *Phys. Rev. B: Condens. Matter Mater. Phys.*, 2011, **83**, 205425.

140 S. Kurth, G. Stefanucci, C. O. Almbladh, A. Rubio and E. K. U. Gross, *Phys. Rev. B: Condens. Matter Mater. Phys.*, 2005, **72**, 035308.

141 X. Zheng, F. Wang, C. Y. Yam, Y. Mo and G. Chen, *Phys. Rev. B: Condens. Matter Mater. Phys.*, 2007, **75**, 195127.

142 G. Stefanucci and C.-O. Almbladh, *Phys. Rev. B: Condens. Matter Mater. Phys.*, 2004, **69**, 195318.

143 J. K. Viljas, F. Pauly and J. C. Cuevas, *Phys. Rev. B: Condens. Matter Mater. Phys.*, 2008, **77**, 155119.

144 J. K. Viljas, F. Pauly and J. C. Cuevas, *Phys. Rev. B: Condens. Matter Mater. Phys.*, 2008, **77**, 155119.

145 P. Myöhänen, A. Stan, G. Stefanucci and R. van Leeuwen, *Phys. Rev. B: Condens. Matter Mater. Phys.*, 2009, **80**, 115107.

146 J. Lehmann, S. Kohler, V. May and P. Hänggi, *J. Chem. Phys.*, 2004, **121**, 2278–2288.

147 I. Franco, M. Shapiro and P. Brumer, *J. Chem. Phys.*, 2008, **128**, 244905.

148 O. Entin-Wohlman, Y. Levinson and Y. M. Galperin, *Phys. Rev. B: Condens. Matter Mater. Phys.*, 2000, **62**, 7283–7288.

149 Y. M. Galperin, O. Entin-Wohlman and Y. Levinson, *Phys. Rev. B: Condens. Matter Mater. Phys.*, 2001, **63**, 153309.

150 J. Bardeen, *Phys. Rev. Lett.*, 1961, **6**, 57.

151 T.-H. Park and M. Galperin, *Phys. Rev. B: Condens. Matter Mater. Phys.*, 2011, **84**, 075447.

152 In eqn (2), a typo in eqn (43) of ref. 151 has been corrected. Specifically, J_k has been replaced by J_{-k}.

153 I. S. Gradshteyn and I. M. Ryzhik, *Table of integrals, series, and products*, Academic Press, San Diego, 2000.

154 W. D. Tian, S. Datta, S. H. Hong, R. Reifenberger, J. I. Henderson and C. P. Kubiak, *J. Chem. Phys.*, 1998, **109**, 2874–2882.

155 R. M. Metzger, *Acc. Chem. Res.*, 1999, **32**, 950–957.

156 R. M. Metzger, *J. Solid State Chem.*, 2002, **168**, 696–711.

157 A. Aviram and M. A. ratner, *Chem. Phys. Lett.*, 1974, **29**, 277.

158 D. R. Ward, F. Huser, F. Pauly, J. C. Cuevas and D. Natelson, *Nat. Nanotechnol.*, 2010, **5**, 732–736.

159 R. Arielly, A. Ofarim, G. Noy and Y. Selzer, *Nano Lett.*, 2011, **11**, 2968–2972.

160 L. P. Kouwenhoven, A. T. Johnson, N. C. van der Vaart, C. J. P. M. Harmans and C. T. Foxon, *Phys. Rev. Lett.*, 1991, **67**, 1626–1629.

161 M. Switkes, C. M. Marcus, K. Campman and A. C. Gossard, *Science*, 1999, **283**, 1905–1908.

162 B. L. Altshuler and L. I. Glazman, *Science*, 1999, **283**, 1864–1865.

163 I. Franco and P. Brumer, *J. Phys. B: At., Mol. Opt. Phys.*, 2008, **41**, 074003.

164 I. Franco, M. Shapiro and P. Brumer, *Phys. Rev. Lett.*, 2007, **99**, 126802.

165 I. Franco, M. Shapiro and P. Brumer, *J. Chem. Phys.*, 2008, **128**, 244905–244913.

166 P. Brune, C. Bruder and H. Schoeller, *Phys. Rev. B: Condens. Matter Mater. Phys.*, 1997, **56**, 4730–4736.

167 M. Moskalets and M. Büttiker, *Phys. Rev. B: Condens. Matter Mater. Phys.*, 2002, **66**, 205320.

168 B. Wang, J. Wang and H. Guo, *Phys. Rev. B: Condens. Matter Mater. Phys.*, 2002, **65**, 073306.

169 T. H. Stoof and Y. V. Nazarov, *Phys. Rev. B: Condens. Matter Mater. Phys.*, 1996, **53**, 1050–1053.

170 B. L. Hazelzet, M. R. Wegewijs, T. H. Stoof and Y. V. Nazarov, *Phys. Rev. B: Condens. Matter Mater. Phys.*, 2001, **63**, 165313.

171 S. Kohler, J. Lehmann, S. Camalet and P. Hänggi, *Isr. J. Chem.*, 2002, **42**, 135.

172 A. Garcia-Martin, D. R. Ward, D. Natelson and J. C. Cuevas, *Phys. Rev. B: Condens. Matter Mater. Phys.*, 2011, **83**, 56.

173 R. R. Chance, A. Prock and R. Silbey, *Adv. Chem. Phys.*, 1978, **37**, 1.

174 It is interesting to note that this energy transfer interaction, which is usually disregarded in standard models of electronic conduction of nanojunctions, can sometimes have important effects on the transport properties of such systems even in the absence of light[175].

175 M. Galperin, A. Nitzan and M. A. Ratner, *Phys. Rev. Lett.*, 2006, **96**, 166803.

176 G. D. Mahan, *Many-particle physics*, Plenum press, New York, 2000.

177 T. Holstein, *Ann. Phys. (N.Y., NY, U.S.)*, 1959, **8**, 325.

178 I. G. Lang and Y. A. Firsov, *Sov. Phys. JETP (Engl. Transl.)*, 1963, **16**, 1301.

179 M. Galperin, A. Nitzan and M. A. Ratner, *Phys. Rev. B: Condens. Matter Mater. Phys.*, 2006, **73**, 045314.

180 S. Mukamel, *Principles of Nonlinear optical Spectroscopy*, Oxford Univ Press, Oxford, 1995.

181 The derivation of eqn (21) relies on the non-crossing approximation (*i.e.* the process *B* is not mixed with other processes in the system; usually justifiable by timescale separation arguments) and on approximate treatments (*e.g.* the Condon approximation or low order perturbation theory) for non-quadratic interaction terms in the molecular Hamiltonian.

182 Eqn (21) is identical to eqn (40) of ref. 136, albeit with a different notation.

183 A general theory of the optical response of a molecule open to electron reservoirs under bias and during current flow is still under development. An obvious difficulty in describing non-equilibrium transport and optical scattering processes on the same footing is that the NEGF formalism, usually employed in descriptions of the non-equilibrium transport, deals with one-to-all transitions (sum over all possible final states for a given initial state) while optical processes are scattering processes with specified initial and final states. Identifying absorption with the flux (22) is valid for a weak near resonant incident field (consistent with the RWA approximation employed in eqn (9e)) where multi-photon processes can be disregarded), where the

photon flux may be equivalently presented by the corresponding intra-molecular electron transitions. An alternative calculation that focuses directly on the photon flux has been presented in ref. 138.

184 E. S. Carmichael, J. B. Ballard, J. W. Lyding and M. Gruebele, *J. Phys. Chem. C*, 2007, **111**, 3314–3321.

185 Y. Meir and N. S. Wingreen, *Phys. Rev. Lett.*, 1992, **68**, 2512–2515.

186 M. Shapiro and P. Brumer, *Quantum Control of Molecular Processes*, Wiley, New York, 2012.

187 L. Allen and J.-H. Eberly, *Optical Resonance and Two-Level Atoms*, Wiley, New York City, 1975.

188 N. V. Vitanov, T. Halfmann, B. W. Shore and K. Bergmann, *Annu. Rev. Phys. Chem.*, 2001, **52**, 763.

189 A. Taflove and S. C. Hagness, *Computational electrodynamics: the finite-difference time-domain method*, Artech House, Norwood, MA, 2005.

190 J. M. Villas-Boas, A. O. Govorov and S. E. Ulloa, *Phys. Rev. B: Condens. Matter Mater. Phys.*, 2004, **69**, 125342.

191 B. Fainberg and A. Nitzan, *Phys. Status Solidi*, 2009, **206**, 948–951.

192 M. Y. Sumetskii and M. L. Fel'shtyn, *JETP Lett.*, 1991, **53**, 24–27.

193 A. Zrenner, E. Beham, S. Stufler, F. Findeis, M. Bichler and G. Abstreiter, *Nature*, 2002, **418**, 612–614.

194 R. Volkovich and U. Peskin, *Phys. Rev. B: Condens. Matter Mater. Phys.*, 2011, **83**, 033403.

195 M. Galperin, M. A. Ratner and A. Nitzan, *Nano Lett.*, 2009, **9**, 758–762.

196 M. Galperin, M. A. Ratner and A. Nitzan, *J. Chem. Phys.*, 2009, **130**, 144109.

197 R. Berndt, J. K. Gimzewski and P. Johansson, *Phys. Rev. Lett.*, 1991, **67**, 3796–3799.

198 R. Berndt, J. K. Gimzewski and R. R. Schlittler, *Ultramicroscopy*, 1992, **42**, 355–359, and referencestherein.

199 Smolyaninov, II and O. Keller, *Surf. Sci.*, 1995, **333**, 1310–1316.

200 A. Downes and M. E. Welland, *Appl. Phys. Lett.*, 1998, **72**, 2671–2673.

201 Y. Suzuki, H. Minoda and N. Yamamoto, *Surf. Sci.*, 1999, **438**, 297–304.

202 N. Nilius, N. Ernst, H. J. Freund and P. Johansson, *Phys. Rev. B: Condens. Matter Mater. Phys.*, 2000, **61**, 12682–12685.

203 M. Iwami, Y. Uehara and S. Ushioda, *Jpn. J. Appl. Phys., Part 1*, 2000, **39**, 4912–4913.

204 M. Iwami, Y. Uehara and S. Ushioda, *Appl. Surf. Sci.*, 2001, **169**, 188–192.

205 A. Olkhovets, S. Evoy and H. G. Craighead, *Surf. Sci.*, 2000, **453**, L299–L302.

206 G. Hoffmann, J. Kliewer and R. Berndt, *Phys. Rev. Lett.*, 2001, **87**, 176803.

207 M. G. Boyle, J. Mitra and P. Dawson, *Nanotechnology*, 2009, **20**, 335202.

208 P. Bharadwaj, A. Bouhelier and L. Novotny, *Phys. Rev. Lett.*, 2011, **106**, 226802.

209 P. Johansson, R. Monreal and P. Apell, *Phys. Rev. B: Condens. Matter Mater. Phys.*, 1990, **42**, 9210–9213.

210 B. N. J. Persson and A. Baratoff, *Phys. Rev. Lett.*, 1992, **68**, 3224.

211 Y. Uehara, Y. Kimura, S. Ushioda and K. Takeuchi, *Jpn. J. Appl. Phys., Part 1*, 1992, **31**, 2465–2469.

212 A. Downes, M. E. Taylor and M. E. Welland, *Phys. Rev. B: Condens. Matter Mater. Phys.*, 1998, **57**, 6706.

213 P. Johansson, *Phys. Rev. B: Condens. Matter Mater. Phys.*, 1998, **58**, 10823–10834.

214 J. Aizpurua, S. P. Apell and R. Berndt, *Phys. Rev. B: Condens. Matter Mater. Phys.*, 2000, **62**, 2065.

215 J. Aizpurua, G. Hoffmann, S. P. Apell and R. Berndt, *Phys. Rev. Lett.*, 2002, **89**, 156803.

216 T. Yokoyama and Y. Takiguchi, *Surf. Sci.*, 2001, **482**, 1163–1168.

217 M. Sakurai, C. Thirstup and M. Aono, *Phys. Rev. Lett.*, 2004, **93**, 046102.

218 E. Flaxer, O. Sneh and O. Cheshnovsky, *Science*, 1993, **262**, 2012–2014.

219 R. Berndt, R. Gaisch, J. K. Gimzewski, B. Reihl, R. R. Schlittler, W. D. Schneider and M. Tschudy, *Science*, 1993, **262**, 1425–1427.

220 F. Touhari, E. J. A. J. Stoffels, J. W. Gerritsen, H. v. Kempen and P. Callant, *Appl. Phys. Lett.*, 2001, **79**, 527–529.

221 Z. C. Dong, A. Kar, Z. Q. Zou, T. Ohgi, P. Dorozhkin, D. Fujita, S. Yokoyama, T. Terui, T. Yamada, T. Kamikado, M. N. Zhou, S. Mashiko and T. Okamoto, *Jpn. J. Appl. Phys., Part 1*, 2002, **41**, 4898–4902.

222 G. Hoffmann, L. Libioulle and R. Berndt, *Phys. Rev. B: Condens. Matter Mater. Phys.*, 2002, **65**, 212107.

223 K. Sakamoto, K. Meguro, R. Arafune, M. Satoh, Y. Uehara and S. Ushioda, *Surf. Sci.*, 2002, **502**, 149–155.

224 X. L. Guo, Z. C. Dong, A. S. Trifonov, S. Yokoyama, S. Mashiko and T. Okamoto, *Jpn. J. Appl. Phys., Part 1*, 2003, **42**, 6937–6940.

225 G. Hoffmann, R. Berndt and P. Johansson, *Phys. Low-Dimens. Semicond. Struct.*, 2003, **3–4**, 209–219.

226 X. H. Qiu, G. V. Nazin and W. Ho, *Science*, 2003, **299**, 542–546.

227 X. L. Guo, Z. C. Dong, A. S. Trifonov, S. Yokoyama, S. Mashiko and T. Okamoto, *Appl. Phys. Lett.*, 2004, **84**, 969–971.

228 M. Sakurai, C. Thirstrup and M. Aono, *Surf. Sci.*, 2003, **526**, L123–L126.

229 Y. Uehara and S. Ushioda, *Phys. Rev. Lett.*, 2004, **92**, 066102.

230 S. Katano, S. Ushioda and Y. Uehara, *J. Phys. Chem. Lett.*, 2010, **1**, 2763–2768.

231 N. L. Schneider, F. Matino, G. Schull, S. Gabutti, M. Mayor and R. Berndt, *Phys. Rev. B: Condens. Matter Mater. Phys.*, 2011, **84**, 153403.

232 Z. C. Dong, A. Kar, R. Dorozhkin, K. Amemiya, T. Uchihashi, S. Yokoyama, I. Kamikado, S. Mashiko and T. Okamoto, *Thin Solid Films*, 2003, **438**, 262–267.

233 Z. C. Dong, A. S. Trifonov, X. L. Guo, K. Amemiya, S. Yokoyama, T. Kamikado, T. Yamada, S. Mashiko and T. Okamoto, *Surf. Sci.*, 2003, **532**, 237–243.

234 M. J. Romero and J. van de Lagemaat, *Phys. Rev. B: Condens. Matter Mater. Phys.*, 2009, **80**, 115432–115435.

235 Y. Zhang, X. Tao, H. Y. Gao, Z. C. Dong, J. G. Hou and T. Okamoto, *Phys. Rev. B: Condens. Matter Mater. Phys.*, 2009, **79**, 075406.

236 X. Tao, Z. C. Dong, J. L. Yang, Y. Luo, J. G. Hou and J. Aizpurua, *J. Chem. Phys.*, 2009, **130**, 084706–084708.

237 G. Tian and Y. Luo, *Phys. Rev. B: Condens. Matter Mater. Phys.*, 2011, **84**, 205419.

238 J. Buker and G. Kirczenow, *Phys. Rev. B: Condens. Matter Mater. Phys.*, 2002, **66**, 245306.

239 U. Harbola, J. B. Maddox and S. Mukamel, *Phys. Rev. B: Condens. Matter Mater. Phys.*, 2006, **73**, 075211.

240 J. S. Seldenthuis, H. S. J. van der Zant, M. A. Ratner and J. M. Thijssen, *Phys. Rev. B: Condens. Matter Mater. Phys.*, 2010, **81**, 205430.

241 S. W. Wu, G. V. Nazin and W. Ho, *Phys. Rev. B: Condens. Matter Mater. Phys.*, 2008, **77**, 205430.

242 G. Hoffmann, R. Berndt and P. Johansson, *Phys. Rev. Lett.*, 2003, **90**, 046803.

243 G. Schull, N. Neel, P. Johansson and R. Berndt, *Phys. Rev. Lett.*, 2009, **102**, 057401–057404.

244 Z. C. Dong, X. L. Guo, A. S. Trifonov, P. S. Dorozhkin, K. Miki, K. Kimura, S. Yokoyama and S. Mashiko, *Phys. Rev. Lett.*, 2004, **92**, 086801.

245 Z. C. Dong, X. L. Zhang, H. Y. Gao, Y. Luo, C. Zhang, L. G. Chen, R. Zhang, X. Tao, Y. Zhang, J. L. Yang and J. G. Hou, *Nat. Photonics*, 2010, **4**, 50–54.

246 F. Xu, F. Haupt and W. Belzig, *Shot-noise of tunnel current coupled to a local plasmon*, Dresden, 2011.

247 J. Tobiska, J. Danon, I. Snyman and Y. V. Nazarov, *Phys. Rev. Lett.*, 2006, **96**, 096801.

248 N. L. Schneider, G. Schull and R. Berndt, *Phys. Rev. Lett.*, 2010, **105**, 026601.

249 *Surface-Enhanced Raman Scattering – Physics and Applications*, ed. K. Kneipp, M. Moskovits and H. Kneipp, Springer, Berlin/Heidelberg, 2006.

250 J. Jiang, K. Bosnick, M. Maillard and L. Brus, *J. Phys. Chem. B*, 2003, **107**, 9964–9972.

251 B. N. J. Persson, *Chem. Phys. Lett.*, 1981, **82**, 561–565.

252 J. R. Lombardi, R. L. Birke, T. Lu and J. Xu, *J. Chem. Phys.*, 1986, **84**, 4174–4180.

253 J. R. Lombardi and R. L. Birke, *J. Chem. Phys.*, 2007, **126**, 244709.

254 M. Oren, M. Galperin and A. Nitzan, *Phys. Rev. B*, 2012, **85**, 115435.

255 J. H. Tian, B. Liu, X. L. Li, Z. L. Yang, B. Ren, S. T. Wu, N. J. Tao and Z. Q. Tian, *J. Am. Chem. Soc.*, 2006, **128**, 14748–14749.

256 T. Dadosh, PhD thesis, Weizmann Institute, 2007.

257 A. M. Nowak and R. L. McCreery, *J. Am. Chem. Soc.*, 2004, **126**, 16621–16631.

258 Q. Zhou, X. W. Li, Q. Fan, X. X. Zhang and J. W. Zheng, *Angew. Chem., Int. Ed.*, 2006, **45**, 3970–3973.

259 Q. Zhou, G. Zhao, Y. W. Chao, Y. Li, Y. Wu and J. W. Zheng, *J. Phys. Chem. C*, 2007, **111**, 1951–1954.

260 W.-H. Park and Z. H. Kim, *Nano Lett.*, 2010, **10**, 4040–4048.

261 H. P. Yoon, M. M. Maitani, O. M. Cabarcos, L. Cai, T. S. Mayer and D. L. Allara, *Nano Lett.*, 2010, **10**, 2897–2902.

262 Z. Liu, S. Y. Ding, Z. B. Chen, X. Wang, J. H. Tian, J. R. Anema, X. S. Zhou, D. Y. Wu, B. W. Mao, X. Xu, B. Ren and Z. Q. Tian, *Nat. Commun.*, 2011, **2**, 305.

263 R. C. Maher, L. F. Cohen, E. C. L. Ru and P. G. Etchegoin, *Faraday Discuss.*, 2006, **132**, 77–83.

264 D. R. Ward, D. A. Corley, J. M. Tour and D. Natelson, *Nat. Nanotechnol.*, 2011, **6**, 33–38.

265 $J_{\nu_i \to \nu_f}$ is related to $J_{i \to f}$ defined below eqn (32) by a multiplicative factor that is proportional to $\rho_R(\nu_i)\rho_R(\nu_f)$, where $\rho_R(\nu)$ is the density of radiation field modes at frequency ν. The factors $(\nu_i \pm \omega_\nu)^4$ correct for the frequency dependence of the outgoing radiation field density of modes and the molecule-radiation field coupling. In ref. 195, 266 and 267 only the density of modes dependence was taken into account so factors $(\nu_i \pm \omega_\nu)^3$ were used. For the parameters used this makes only marginal dependence on the resulting Raman temperature.

266 M. Galperin and A. Nitzan, *J. Phys. Chem. Lett.*, 2011, **2**, 2110–2113.

267 M. Galperin and A. Nitzan, *Phys. Rev. B: Condens. Matter Mater. Phys.*, 2011, **84**, 195325.

268 A. G. Brolo, A. C. Sanderson and A. P. Smith, *Phys. Rev. B: Condens. Matter Mater. Phys.*, 2004, **69**, 045424–045429.

269 R. C. Maher, L. F. Cohen, P. Etchegoin, H. J. N. Hartigan, R. J. C. Brown and M. J. T. Milton, *J. Chem. Phys.*, 2004, **120**, 11746–11753.

270 T. H. Park and M. Galperin, *EPL*, 2011, **95**, 27001.

271 Note that the presentation, starting from the model (7)–(9), focuses on a single optical transition between two given molecular energy levels, as appropriate for resonance Raman scattering, already implied by the use of the rotating wave approximation in the model. While the formalism can be easily extended to a multilevel system, *e.g.* eqn (28) is replaced by $J_\alpha = - \sum_{m,m'} \int_{-\infty}^{\infty} dt [\Pi_\alpha^{<}(-t)\mathscr{G}_{mm'}^{>}(t) - \Pi_\alpha^{>}(-t)\mathscr{G}_{mm'}^{<}(t)]$ with the sum going over all relevant pairs of molecular levels, different considerations are more appropriate when the incident radiation is not in resonance with a molecular transition, see *e.g.*, ref. 254.

272 H. Haug and A.-P. Jauho, *Quantum Kinetics in Transport and Optics of Semiconductors*, Springer, Berlin, 1996.

273 L. V. Keldysh, *Sov. Phys. JETP (Engl. Transl.)*, 1965, **20**, 1018.

274 M. Galperin, M. Ratner and A. Nitzan, *Phys. Rev. B: Condens. Matter Mater. Phys.*, 2007, **75**, 155312.

275 The difference between the two temperature estimates at low bias partly reflects the large error associated with the Raman estimate, resulting from the very small anti-Stokes component at low temperature.

276 M. Galperin, K. Saito, A. V. Balatsky and A. Nitzan, *Phys. Rev. B: Condens. Matter Mater. Phys.*, 2009, **80**, 115427.

277 J. I. Gersten, R. L. Birke and J. R. Lombardi, *Phys. Rev. Lett.*, 1979, **43**, 147.

278 A. Otto and M. Futamata, in *Surface-Enhanced Raman Scattering Physics and Applications*, Springer, NYC, 2006, vol. 103, pp. 147–182.

279 J. R. Lombardi, R. L. Birke, L. A. Sanchez, I. Bernard and S. C. Sun, *Chem. Phys. Lett.*, 1984, **104**, 240–247.

280 J. R. Lombardi and R. L. Birke, *J. Phys. Chem. C*, 2008, **112**, 5605–5617.

This journal is © the Owner Societies 2012

Phys. Chem. Chem. Phys., 2012, **14**, 9421–9438 | 9437

281 J. R. Lombardi and R. L. Birke, *Acc. Chem. Res.*, 2009, **42**, 734–742.

282 D. P. Fromm, A. Sundaramurthy, A. Kinkhabwala, P. J. Schuck, G. S. Kino and W. E. Moerner, *J. Chem. Phys.*, 2006, **124**, 061101.

283 L. Cui, D. Y. Wu, A. Wang, B. Ren and Z. Q. Tian, *J. Phys. Chem. C*, 2010, **114**, 16588–16595.

284 S. M. Morton and L. Jensen, *J. Am. Chem. Soc.*, 2009, **131**, 4090–4098.

285 S. M. Morton, D. W. Silverstein and L. Jensen, *Chem. Rev.*, 2011, **111**, 3962–3994.

286 D. M. Newns, *Phys. Rev.*, 1969, **178**, 1123.

287 P. Song, P. Nordlander and S. Gao, *J. Chem. Phys.*, 2011, **134**, 074701–074705.